POST-HARVEST PREDICTION OF TENDERNESS IN PORK

A Thesis

by

KYLE MATTHEW SEGNER

Submitted to the Office of Graduate Studies of
Texas A&M University
in partial fulfillment of the requirements for the degree of

MASTER OF SCIENCE

May 2011

Major Subject: Animal Science

Post-harvest Prediction of Tenderness in Pork

POST-HARVEST PREDICTION OF TENDERNESS IN PORK

A Thesis

by

KYLE MATTHEW SEGNER

Submitted to the Office of Graduate Studies of
Texas A&M University
in partial fulfillment of the requirements for the degree of

MASTER OF SCIENCE

Approved by:

Co-Chairs of Committee,	Jeffrey W. Savell
	Rhonda K. Miller
Committee Member,	Daniel S. Hale
Head of Department,	Gary Acuff

May 2011

Major Subject: Animal Science

ABSTRACT

Post-Harvest Prediction of Tenderness in Pork.

(May 2011)

Kyle Matthew Segner, B.S., Texas A&M University

Co-Chairs of Advisory Committee: Dr. Jeffrey W. Savell
Dr. Rhonda K. Miller

As variation in pork tenderness has increased, identification of tenderness has become an industry need. This study consisted of 1208 pork loins randomly selected to test the efficacy of four automated grading techniques. Visible and near-infrared spectroscopy (VVNIR) (350-1830 nm wavelengths), bioelectrical impedance (EI) (resistance, reactance, phase angle, and partial capacitance), pH, and CIE L*, a* and b* color space values were used to predict chemical moisture and lipid, pH, Warner-Bratzler shear force (WBSF), and Slice shear force (SSF) on 13 d aged pork loins. The means and standard deviations for WBSF were (22.95 and 5.16) and SSF were (165.49 and 58.15). Prediction was based on stepwise linear regression and partial least squares regression. VNIR, pH, and color, when in combination, had the highest R^2 (0.19 and 0.21) for the prediction of WBSF and SSF, respectively. Partial least squares regression (PLSR) was used to remove autocorrelation between VNIR values. By using PLSR, with an R^2 value of 0.49, 100 % of the "tender" chops were correctly classified, 93 % of the "intermediate" chops were correctly classified, and 92% of the "tough" chops were correctly classified into its category for WBSF. However, SSF was much lower (R^2 =

0.24) with only correctly placing 62 % of the “tender” chops and only 48 % of the “intermediate” and “tough” chops. Electrical impedance, alone or in combination with other technologies, either did not improve predictability of linear regression equations (increase R^2) or of PLSR models (increase R^2). Equations and models that included EI values had low R^2. When adding EI to the regression equation involving all variables, R^2 increased slightly from 0.19 to 0.21 in predicting WBSF, and from 0.21 to 0.25 for SSF. When pH or CIE L* color space values were included in linear regression or PLSR models to predict WBSF and SSF, R^2 values increased from 0.14 to 0.19 for WBSF, and 0.14 to 0.21 for SSF. pH played a large role in predicting WBSF and SSF, along with CIE L*. Thus, for an on-line situation, use of VNIR, pH, and color could be used to predict tenderness. Utilization of VNIR alone could be effective in predicting pork tenderness (WBSF). Using EI alone, or in combination with VNIR, would not provide acceptable prediction of WBSF or SSF. Use of VNIR with pH and color would improve the ability to predict tender and intermediate pork WBSF and SSF, but the additional improvement in accuracy may not be warranted based on the cost and additional time needed when using more than one technology.

TABLE OF CONTENTS

LIST OF FIGURES

LIST OF TABLES

Page

Page

CHAPTER I

INTRODUCTION

Pork tenderness may not have been a issue until the results of the Pork Quality Benchmark Consumer study (Moeller et al., 2010) was completed, automated grading for pork quality has emphasized either pH or color as quality predictions. Structurally, pork and beef are highly similar, whereas differences exist. It is reasonable to assume that some of the chemical and mechanical factors used to predict tenderness in beef may provide information when developing a system to predict tenderness in pork. This research used existing technology that was recently developed for beef tenderness prediction and examined the efficacy of these technologies for pork tenderness prediction. In this research visible and near-infrared spectroscopy (VNIR), electrical impedance (EI), pH, and color were used as predictors of tenderness. Therefore, the hypothesis was that singly or in combination, VNIR, EI, pH, and/or Minolta CIE L*, a* and b* color space values can predict pork tenderness assessed either as Slice shear force or Warner-Bratzler shear force.

To test these hypotheses, 1208 pork loins were randomly selected from 4 major pork harvest processing plants. These pork loins would be assessed by the 4 instruments (VNIR, EI, pH, and Minolta colorimeter) and the Slice shear force, Warner-Bratzler shear force, chemical lipid and chemical moisture would be determined. Linear stepwise

---

This thesis follows the style of *Meat Science*.

Regression and partial least squares regression would be used to develop prediction equations. The second hypothesis was that these same instruments except pH can be used to predict together or in combination meat pH. The third hypothesis was that these four instruments, alone or in combination, could predict chemical lipid or chemical moisture. The second and third hypothesis used the same instruments to predict tenderness, pH and/ or chemical lipid, and would provide an all inclusive automated grading system for pork processors to address all three major quality issues.

CHAPTER II

LITERATURE REVIEW

Historically, pork *M. longissimus* has been considered to be relatively tender (DeVol et al., 1988). However, some studies contradict the assumption that pork is uniformly tender. It has been reported that there was significant animal-to-animal variation in pork tenderness (Davis, Smith, Carpenter, & Cross, 1975; DeVol et al., 1988). Furthermore, recent emphasis in the U.S. on selection for increased lean growth in pork has been associated with unfavorable changes in the rate of postmortem pH decline, PSE effects, and tenderness (Lonergan, Huff-Lonergan, Rowe, Kuhlers, & Jungst, 2001). Also, the most recent Pork Quality Benchmark (Moeller et al., 2010) showed variation in pork loin pH and tenderness. Cameron (1990) found that with selection for increased carcass lean weight, the meat becomes less tasty, less juicy, less tender, and lower in overall acceptability. To ensure high eating quality and to produce a more consistent product in pork, the industry has relied on “enhancing” the product by the addition of a solution of phosphates, salt, and sometimes flavorings (Brewer, Jensen, Prestat, Zhu, & McKeith, 2002). This approach has been relatively successful. However, there are growing indications that the demand for non-enhanced pork products is increasing and would be considered a premium product. Thus, the ability to select pork that is “naturally” tender within a non-enhanced product line might increase the marketing opportunities for pork.

Consumer research supported by the National Pork Board has identified that pork tenderness impacts consumer acceptance (Moeller et al., 2010). This research documented that pH impacted consumer acceptance, and that pork tenderness was more highly related to consumer acceptance than pork color or cooked temperature endpoint. The pork industry has focused most pork quality research on decreasing variation in meat pH, improving pork meat color, and increasing marbling. Whereas some research has examined pork tenderness, pork tenderness has not been a major focus as a pork quality trait. Pork tenderness, measured by Warner-Bratzler shear force (WBSF), was shown to vary in non-enhanced pork loins (n=678) from 1.23 to 7.01 kg in the Pork Quality Benchmark study (Moeller et al., 2010). This study also showed that tenderness was affected by increased cooked endpoint temperature. Van Laack, Stevens & Stalder (2001) conducted a study to evaluate the effects of ultimate pH, intramuscular fat, and storage time on the tenderness of pork *M. longissimus* and determined whether the contribution of the various factors were dependent on genetic lines (Berkshire, Duroc, and Hampshire boars crossed with Yorkshire-Landrace sows). In this study, they showed that at d 2 the Hampshire pork had a lower ($P< 0.05$) WBSF than the other pork; however, this difference disappeared at d 7. Due to glycolytic potential, the 30 Hampshire pigs that were carriers of the Rendment Napole gene were excluded from the analysis. The relationship between ultimate pH and WBSF, it was different for each cross: in Duroc pork it was quadratic, in Hampshire pork WBSF increased linearly, and in Berkshire pork there was no significant relationship. For the correlation between lipid and WBSF was -0.11 at d 2, -0.21 at d 7, and -0.19 at d 14.Percent lipid does play a role in WBSF, as percent of lipid increased the WBSF decreased, but this relationship was not strong in pork and may not appreciably impact tenderness except when lipid varies greatly.

The beef industry has emphasized beef tenderness as an important consumer acceptance trait, and research to assess beef tenderness using automated grading instruments has been conducted for many years. Computer vision is a rapid, economic, consistent and objective inspection technique, which has expanded into many diverse industries such as agricultural and food industry with the inspection and grading of fruit, vegetables, and meat products (Brosnan, & Sun, 2002). The major technologies examined or implemented by the beef industry include electrical impedance, camera visioning technology, visible and near-infrared reflectance, and ultrasound. Visioning technology and ultrasound have been extensively evaluated by the pork industry as predictors of meat color, pH, or marbling (Hoving-Bolink et al., 2005; Liao, Fan, & Cheng, 2010). The pork industry has an opportunity to utilize existing instrumentation and to examine the use of either a single or multiple instruments to predict pork tenderness. This project utilized four instruments, Visible and near-infrared spectroscopy (VNIR), electrical impedance (EI), pH, and CIE color space (L*, a*, and b*) values to depict pork tenderness.

VNIR Spectra Analysis

VNIR has been extensively studied for prediction of beef tenderness (Bowling et al., 2009; Price, Hilton, VanOverbeke, & Morgan, 2008; Shackelford, Wheeler, & Koohmaraie, 2005). It has been found that VNIR instrumentation provided a highly repeatable on-line spectroscopic evaluation of beef quality traits to classify beef carcasses for tenderness. Shackelford et al. (2005) conducted an experiment to segregate 146 beef carcasses in classes of tough and tender within the US Select carcass grade: VNIR spectroscopy (VISNIR) (552-930 nm wavelengths) was used as an online application to predict the tenderness on *M. longissimus.* Steaks on d 14 post-harvest were cooked using a belt grill and Slice shear force was measured. Shackelford et al. (2005) found that the most variation in Slice shear force that could be accounted for by the amount of light reflected at any single wavelength was 9.6%. However, with a 10-variable regression equation, they accounted for 38% of the variation in Slice shear force in the validation data set. For this study, it was determined that VNIR instrumentation would be a viable technology for industry beef tenderness prediction.

Two VNIR instruments from Analytical Spectra Devices, Inc. (Boulder, CO) have been developed for prediction of beef tenderness. While both instruments are manufactured by the same company, they were developed by different research institutions. The first instrument was developed by researchers at the USDA, ARS Roman L. Hruska U.S. Meat Animal Research Center in Clay Center, NE (Shackelford et al., 2005). The second instrument was developed by researchers at Oklahoma State University (Price et al., 2008; Rust et al., 2008). Both instruments are being used in beef commercial processing plants in on-line situations to assess beef tenderness. While these instruments use the same technology, they use different algorithms to predict beef tenderness category (tough versus tender). Price et al. (2008) found that their VNIR system (400-2500 nm wavelengths) showed a low correlation when using VNIR to predict Slice Shear force classifications. However, when using their VNIR system to identify the carcasses into tender (Slice Shear force < 25 kg) or tough (Slice Shear force > 25 kg) categories, the VIS-NIR system correctly classified 26 out of 28 (92.9% accuracy) carcasses as “tough.” Rust et al. (2008) found that they correctly classified 20 “tough” carcasses into the “not certified tender” category out of a total of 39 classified “tough” carcasses.

The above instruments use only selected spectra within the visible and near-infrared range to predict beef tenderness. Analytical Spectrum Devices, Inc. has supported research in Europe and Australia that indicated that information found using a wider bandwidth improved tenderness prediction (personal communication, ASD, Inc., Boulder, CO.). Limited information is available on prediction of pork tenderness using VNIR technology. It is reasonable to hypothesize that VNIR technology could provide information for pork tenderness prediction. As VNIR is a measurement of color and color is related to pork quality and provides some prediction of pork tenderness, use of VNIR technology alone or in a combination with other technologies to predict pork tenderness needs to be evaluated. Analytical Spectrum Devices, Inc. agreed to donate the use of a VNIR instrument that had a wider bandwidth for the use in this study (350-1830 nm wavelengths). It is important to use the wider bandwidth device so that the broad spectrum of data can be used to examine prediction.

Electrical Impedance

Electrical impedance has been used to predict beef palatability (Wulf, & Page, 2000). Wulf and Page (2000) found a correlation between electrical impedance and

WBSF of the *M. longissimus* to be somewhat low, but significant (0.25). The correlation to palatability characteristics (juiciness, flavor intensity and flavor desirability) within three different muscles (*M. longissimus* (0.08, 0.13, and 0.61), *M. luteus medius* (0.33, 0.24, and 0.62), and *M. semimembranosus* (0.18, 0.14, and 0.26)) were also low but significant. When used in a regression model along with color and pH, the values from the impedance system did not improve prediction of beef palatability. A prototype impedance system was developed, and research at South Dakota State University has shown that impedance technology was additive to other technologies such as VNIR in accuracy of tenderness prediction (Nath, 2008). Nath (2008) was able to find fairly high correlations (0.51) to WBSF in beef with the electrical impedance system. By using two components (VNIR and electrical impedance), an R^2 of 0.12 was reported when trying to predict tenderness in beef. The authors concluded that electrical impedance was a weak predictor, but may be useful in the use of predicting beef aging.

Electrical impedance generates four variables: resistance, reactance, phase angle, and partial capacitance. This information has been used to predict human body composition (Lukaski, 1996) and human disease states (Barbosa-Silva, & Barros, 2005). Impedance is the frequency-dependent opposition of a conductor, animate or inanimate, to the flow of an administered alternating electrical current (Lukaski, 1996). This opposition has two components or vectors termed resistance and reactance. Resistance is pure opposition of the conductor to the flow of current, where reactance is the reciprocal of capacitance, or the voltage stored by a condenser for a brief period of time (Lukaski, 1996). Resistance measurements have been shown to predict water content, and reactance measures have been related to cell membrane integrity. Moisture content and cell membrane integrity have been shown to be somewhat related to meat tenderness. Capacitance causes the administered current to lag behind the voltage and creates a phase shift that is represented geometrically as the phase angle or the tangent of the ratio of reactance/ resistance. It is reasonable to hypothesize that those changes in cell membrane integrity or water content may be related to pork tenderness. As pork tenderness is somewhat related to pork meat pH and lipid content (DeVol et al., 1988; Ramsbottom, & Strandine, 1948), the addition of variables to account for these effects on pork tenderness may augment pork tenderness prediction. Also, protein degradation occurs more in low pH pork subjected to rapid pH decline. During the rapid pH decline, body temperature increases as a result of increased metabolism. This increased temperature increases protein denaturation (Watanabe, Daly, & Devine, 1996), and this physiological phenomenon has been shown to alter membrane integrity (Yu, & Lee, 1986). Swantek, Crenshaw, Marchello and Lukaski (1992) showed that when pork carcass length^2 was divided by resistance or reactance values, a higher correlation ($r = .71$) to percent carcass fat was acquired. While electrical impedance may not independently be highly related to pork tenderness, it may provide information related to water content, cell membrane integrity, and percent fat and subsequently may improve pork tenderness predictions.

pH

Meat tenderness has been shown to be related to the ultimate pH of muscle (Bouton, Harris, & Shorthose, 1971; DeVol et al., 1988; Koohmaraie, 1994). pH has been shown to affect the calpain system, the system that influences post-mortem proteolysis. The calpain-specific inhibitor, calpastatin has been shown to play an important role in influencing tenderization and as a marker for meat quality (Kemp, Sensky, Bardsley, Buttery, & Parr, 2009).

Water holding capacity (WHC) has been known to greatly affect cooked meat tenderness (Gault, 1985). Wismer-Pedersen (1959) found pH to be highly correlated to WHC. As WHC decreased, meaning the amount of loosely bound water increased, pH decreased ($r = -0.71$, $p = 0.001$). Yu and Lee (1986) conducted a study to examine if pH had an effect on beef tenderness. They found that on days 1 and 7 post-harvest, the higher pH (above 6.3) meat was consistently more tender than the low pH meat (below 5.8) and intermediate pH meat (5.8 – 6.3). While knowing that pH could be a useful in predicting tenderness, a study that consisted of 3,435 beef carcasses from animals ranging from 11 to 14 months of age (472 bulls, 978 heifers, and 1985 steers) was conducted (Jeremiah, & Gibson, 1991). They reported that segregation of carcasses based on ultimate pH values was effective in segregating the tough carcasses in all sex groups. DeVol et al. (1988) discovered that when ultimate pH was taken in a random sample of pork carcasses ($n = 120$), that ultimate pH was not strongly correlated to muscle characteristics (pH and color) and palatability attributes. However, pH had a higher correlation with firmness and color ($r = .62$ and $.73$, respectively; $P<0.001$). Moeller et al. (2010) found that pork loin pH and WBSF were the primary contributors to consumer perceptions. They found that an incremental increase in pH (0.20 unit) and decrease in WBSF (4.9 N) resulted in a 4-5% reduction in the consumer ratings on an 8-

point scale. As pH plays a major role in the consumer perceptions of eating quality, pH may be a useful technique in attempting to predict tenderness in pork.

Color

Pale colored pork, defined as light grayish pink, has been linked with extremely undesirable pork quality (Norman, Berg, Heymann, & Lorenzen, 2003). Steenkamp and Van Trijp (1996) showed that pork color greatly impacted quality expectations of the consumer. Davis et al. (1975) showed that color played a major role in segmenting pork loins into groups that differed significantly in juiciness, tenderness, overall satisfaction, and cooking loss percentages. According to Norman et al. (2003), trained sensory panelists found darker colored pork chops to be more tender and juicier than lighter colored pork chops. Wulf, O'Connor, Tatum, and Smith (1997) found WBSF to have the highest correlation to CIE L* and b* color space values in relation to beef tenderness. While color may not be the best indicator alone, Norman et al. (2003) found that pH values in pork had a low, but significant, negative correlation ($P < 0.05$) to WBSF, a* and b* color space values and chroma values, which indicated those chops with a darker color had a higher pH value. However, Moeller et al. (2010) showed that CIE L*, a* and b* were not significant model effects on consumer perceptions compared to that of pH and WBSF.

Knowing that VNIR has the ability to predict tough and tender categories in beef (Shackelford, Wheeler, & Koohmaraie, 1999b), and in combination with EI may be able to increase that prediction ability of tenderness (Nath, 2008). pH being a high predictor of consumer perceptions (Moeller et al., 2010), and color showing to have an effect on pH effects and tenderness (Norman et al., 2003). Utilizing these instruments (VNIR, EI, pH, and color), it would be evident that these four instruments would be great predictors of tenderness in pork and may be able to be used in an online situation.

As VNIR has been shown to be adequately predict tough and tender (Shackelford et al., 2005), it is reasonable to examine the ability of VNIR to predict tenderness in pork. Additionally, use of EI alone or in combination with VNIR may improve tenderness prediction. As pH and color impact consumer perceptions (Moeller et al., 2010), either using pH and instrumental color measurements in pork tenderness prediction. In addition to predicting tenderness, as ph and chemical lipid are important pork quality attributes, this study examined the use of these four technologies, VNIR, EI, pH, and instrumental color, to predict pH and chemical lipid. The ultimate goal of this research was to provide the pork industry with an automated grading system utilizing one or more technologies to adequately predict pork tenderness. However, if the same technologies could predict pork pH and/or chemical lipid, greater utilization and justification of use of these technologies would exist. A third issue is that these technologies have to be adaptable to the pork processing environment and to be used at line speeds in the plants. The technologies addressed in our study meet these criteria.

CHAPTER III

MATERIALS AND METHODS

Sample Collection

Pork carcasses (n=1208) were selected from four pork harvest and processing plants over three selection trips. Approximately 300, 412E pork loins (NAMP, 2010), were selected from each plant and evaluated using the USMARC Noninvasive Tenderness Prediction System (Shackelford et al., 2005). This was used to provide sufficient sampling to assure variation in pork carcass selection and sufficient days to account for instrument usage variability. Loins were removed under industrial conditions (2°C ± 1°C), vacuum-packaged using each individual plant packaging system, and transported under refrigeration to the Roman L. Hruska US Meat Animal Research Center in Clay Center, NE. Loins were stored at 2°C for 13 d post-harvest. On d 13, loins were removed from the vacuum-package.

Chops assigned to instrument assessment were evaluated within 20 minutes post-slicing at 2°C. The VNIR and Impedance data were collected from the "rib," the medial aspect of the *M. longissimus,* an only VNIR was assessed on the "chop" or sliced loin face due to the size of the area in which was available. Before being sliced into 2.54 cm chops, VNIR instrument (Quality Spec BT, ASD Inc., Boulder CO) was calibrated using a white tile. Two readings were taken on the medial aspect of the *M. longissimus* and were referred to as the rib VNIR data. The wavelengths ranged from 350-1830 nm. The EI values were derived from approximately the same location as the VNIR, toward the anterior end of the loin. The four probes of the EI system were placed so that every probe was placed on lean surface, avoiding any fat or connective tissue on the surface.

Slicing began at the anterior end and continued to the posterior end until all 8 chops (2.54 cm) were obtained. The first loin chop removed from the anterior loin end was used for chemical moisture and lipid assessment. This chop then was vacuum-packaged (7500 1830 vacuum bags, oxygen transfer rate 50-70 cc/m²/24h, Koch Inc., Kansas City, MO; 903003 Ultravac 2100, Koch Inc., Kansas City, MO) and frozen (-10°C) before transport. The moisture and lipid chop was transported frozen (-10°C ± 5°C) via cargo van contained in 120 quart ice chests to Texas A&M University for assessment. VNIR was assessed on the second anterior loin chop, the VNIR camera head was placed approximately in the center of the chop and a measurement was taken (chop data). After every 10 samples, the VNIR was recalibrated using a white tile. Two pH values also were assessed using the same chop in two random locations using a pH probe (HI 98240 or HI98140, Hanna Instruments, Italy) and the two values were averaged (loin pH). The pH meter was calibrated using standard buffers at pH 4.0 and pH 7.0 at the start of sampling and was recalibrated after every 2 h. Color CIE (L*, a*, and b* color space values) was assessed using a Minolta Colorimeter (CR-300, 8 mm diameter head, 10° standard observer, D^{65} light source; Minolta Co., Ramsey, NJ) and was calibrated using both white and black tiles. Three readings were obtained from the *M. longissimus* on the same chop that VNIR and pH were determined and values then were averaged. The color values was taken approximately 30 minutes after slicing while temperature was held at 2°C ± 1°C during holding and evaluation.

The six subsequent chops were randomly assigned by location so that two were used for Slice shear force (SSF) and Warner-Bratzler shear force (WBSF), High Resolution Imaging, and Stress-Strain Imaging (SSI). The SSI and High Resolution Imaging (conducted by Colorado State University), chops not part of this study, were always the sequential chops in that they were cut next to each other. The five toughest and five most tender chops per plant based on slice shear force determinations were vacuum-packaged and shipped overnight at 2°C to Dr. Jonathan Ophir at the University of Texas Health Science Center in Houston for evaluation by SSI within four days after arrival. Chops for SSF were cooked and evaluated on d 14. Warner-Bratzler shear force chops were vacuum-packaged and frozen on d 14. Frozen chops (-10°C ± 5°C) were transported via cargo van contained in 120 quart ice chests to Texas A&M University for Warner-Bratzler shear force determinations.

Chemical Assessment

The 2.54 cm thick anterior chops were removed from the vacuum-package, trimmed of all external fat and powdered in liquid nitrogen to make a homogenous sample. The powdered samples were sub-sampled for chemical moisture and chemical lipid using a modified version of the oven-dried ether extraction method described by AOAC (1995). Of the powdered sample, three to four grams were put in a dried, pre-weighed thimbles, and analysis were conducted in triplicates. Whatman filter paper (Whatman filter paper #1 Qualitative Circles, 125 mm; Cat. # 1001 125, VWR International, LLC) was used to make thimbles that were dried for twelve hours at 100°C prior to use. The samples were oven-dried at 100°C for 16-18 h, removed and cooled in desiccators for 30-45 minutes. Samples were reweighed for moisture determination (Percent moisture = (Dried Sample Weight/ Raw Sample Weight) x 100). Lipid determination was conducted by placing 14 to 16 thimbles in a Soxhlet apparatus, the flask below were filled to 1000 ml of petroleum ether and fluxed for 18 h. Once ether extraction was completed, the samples were removed and arranged in a single layer under a hood to allow ether to evaporate completely (approximately 45 minutes). Thimbles were then oven-dried for a minimum of 12 h at 100° C and were reweighed for percent lipid determination (Percent lipid = (Ethered Sample Weight/ Non-ethered Sample Weight) x 100).

Tenderness Assessment

From the two chops that were assigned for WBSF, the chops were weighed prior to and after being broiled on an open top electric grill (Hamilton Beach grill, Hamilton Beach/ Proctor-Silex, Inc., Southern Pines, NC) to an internal temperature of 65°C for WBSF determination. This internal temperature was selected as it represents the new recommended internal temperature for pork chops by the National Pork Board. Additionally, Moeller et al. (2009) showed that the internal temperatures of 68.3, 73.9, and 79.4°C did not differ in WBSF. Internal temperature were monitored with iron constantan thermocouples inserted into the geometric center of each chop (TT-J-36-SLE, Omega Engineering, Inc., Stanford, CT), and temperatures were monitored using hand-held temperature recorders (model HH-21, Omega Engineering, Inc., Stanford, CT). Chops were cooked to the desired temperature with cooking time, temperature, and cooked weight recorded. Cook loss was determined using pre- and post-cooked weights

(Cook Loss = Cooked Chop Weight/ Raw Chop Weight) * 100). Chops were then cooled for four hours to approximately 22.2° C, and then four to six 1.27 cm diameter cores parallel to the longitudinal orientation of the muscle fibers were removed from the two corresponding chops and averaged. Cores were sheared once with a Warner-Bratzler shearing device (United Smart-1 Test System SSTM-500, United Calibration Corp., Huntington Beach, CA) certified by United Testing Systems, Inc. A 1.168 cm Warner-Bratzler stainless steel blade was used to hold cores and head speed of 200 mm/minute was used with a 9.072 kg load cell to segment cores. Cores that were “hour-glass” or not consistent in shape were eliminated from evaluation. Maximum force for each core was recorded in kg, and analyzed as the average of the cores removed from each chop, all averaged values were converted into N from kg for data reporting. The WBSF from the two chops from a loin was averaged as the final WBSF value for a loin.

SSF was conducted at the U.S. Meat Animal Research Center in Clay Center, NE. At 14 d postmortem, the two assigned fresh pork loin chops from each loin were cooked using a Magigrill belt grill (model TBG-60; MagiKitch’n Inc., Quakertown, PA). Cooking with the belt grill and SSF was determined following the procedures developed by (Shackelford, Wheeler, & Koohmaraie, 1999a; Shackelford et al., 1999b; Shackelford, Wheeler, & Koohmaraie, 2004). Belt grill settings (top heat = 163°C, bottom heat = 163°C, preheat = 149°C, height (gap between platens) = 2.16 cm, and cook time = 5.8 min) were designed to achieve a final internal temperature of 71°C for a 2.54 cm thick *M. longissimus* chops. After the chops exited the belt grill, a needle thermocouple probe was inserted into the geometric center of the chop and post-cooking temperature rise was monitored with a handheld thermometer (Cole-Parmer, Vernon Hills, IL). The maximum temperature, which occurred about 2 minute after the chop exited the belt grill, was recorded as the final cooked internal temperature. Immediately after cooking, a 1 cm thick, 5 cm long slice was removed from each steak parallel to the muscle fibers. The slice was acquired by first cutting across the width of the *M. longissimus* at a point approximately 2 cm from the lateral end of the muscle. Using a sample sizer, a cut was made across the *M. longissimus* parallel to the first cut. Using a knife that consisted of two parallel blades spaced 1 cm apart, two parallel cuts were simultaneously made through the length of the 5 cm long chop portion at a 45° angle to the long axis of the *M. longissimus* and parallel with the muscle fibers. Each sample was sheared once with a flat, blunt-end blade using an electronic testing machine (model 4411; Instron Corp. Norwood, MA). The crosshead speed was set at 500 mm/minute using a 100 kg load cell. The values from both chops were recorded in kg, and averaged both values, then converted from kg to N for data analysis.

Data Analysis

Carcasses were ranked according to loin SSF from tender to tough. The first carcass and every other carcass across the entire data set was assigned to the validation data set (n=604). The remainder of the carcasses were assigned to the prediction data set (n=604). The prediction data was used to develop prediction equations and was used to rank order for tenderness (1= most tender to 604= least tender). Descriptive statistics for the validation and prediction data sets were assessed using PROC MEANS of SAS (v9.2, SAS Institute, Cary, NC). The dependent variables were WBSF, SSF, pH, and chemical lipid the independent variables were VNIR wavelengths from 350 nm to 1830 nm, pH, resistance, reactance, phase angle, partial capacitance , and color (CIE *L**, a*, and b* color space values). For the independent VNIR variables, reflectance values from the toughest chop, most tender chop, and the average of all the reflectance values for all chops across the prediction and validation data sets with all wavelengths ranging from 350-1830 nm were plotted in Figure 1. The values of the measured reflectance at each individual peak and valley along the lines were used, along with a calculated difference between each peak and valley in the analysis. The wavelengths that were used were 350 nm, 373 nm, 415 nm, 485 nm, 544 nm, 624 nm, 626 nm, 698 nm, 757 nm, 799 nm, 973 nm, 1001 nm, 1068 nm, 1186 nm, 1271 nm, 1416 nm, and 1830 nm. The differences that were calculated were the change in reflectance values from one point to another; Difference 1 (373 nm – 415 nm), Difference 2 (415 nm – 485 nm), Difference 3 (485 nm – 544 nm), Difference 4 (544 nm – 624), Difference 5 (624 nm -626 nm), Difference 6 (626 nm – 698 nm), Difference 7 (698 nm – 757 nm), Difference 8 (757 nm – 799 nm), Difference 9 (799 nm – 973 nm), Difference 10 (973 nm – 1001 nm), Difference 11 (1001 nm – 1068 nm), Difference 12 (1068 nm – 1186 nm), Difference 13 (1186 nm –

1271 nm), Difference 14 (1271 nm – 1416 nm), and Difference 15 (1416 nm – 1830 nm). The individual wavelengths could not be read into SAS. In order to assess relationships, characterization of the reflectance spectrum by defining points of change, either peak or valley, and the change from peaks to valleys provided information for prediction that would characterize the reflectance values. Additionally, simple correlations coefficients between VNIR reflectance values were high (data not presented), showing high levels of autocorrelation between many of the wavelengths. To understand relationships between variables, simple correlations coefficients were calculated for and between independent and dependent variables using PROC CORR of SAS (v9.2, SAS Institute, Cary, NC). Stepwise regression was conducted to develop linear regression equations using PROC REG of SAS (v9.2, SAS Institute, Cary, NC). The stepwise regression equations were developed to predict WBSF, SSF, pH, moisture and lipid. Parameters for the stepwise regression were variables with $p< 0.15$ could enter the equation. Stepwise linear regression equations were developed using six strategies:

0 VNIR data only; 2) VNIR and pH data; 3) color and pH data; 4) VNIR, color and pH; 5; EI, color and pH; 6) VNIR, EI, color and pH. These equations were developed using VNIR data for chops in the validation data from the chop surface. These strategies were used to determine if one, two, three, or four technologies were needed to predict pork quality.

Due to the high level of autocorrelation between VNIR variables, the validation data were used to develop partial least squares regression (PLSR) models using Unscrambler (The Unscrambler X 10.0.0, CAMO Software Inc., Woodbridge, NJ). The same six strategies were used in developing the PLSR models as for stepwise linear regression. A model was run for the chop data set, and was used to predict WBSF and SSF. The independent variables (VNIR, pH, resistance, reactance, phase angle, partial capacitance, CIE L*, a*, and b* color space values) were ran collectively and in groups of the same origin VNIR, pH, EI (reactance, phase angle, partial capacitance), and color (CIE L*, a*, and b* space values). After applying the six strategies for PLSR, models did not show to

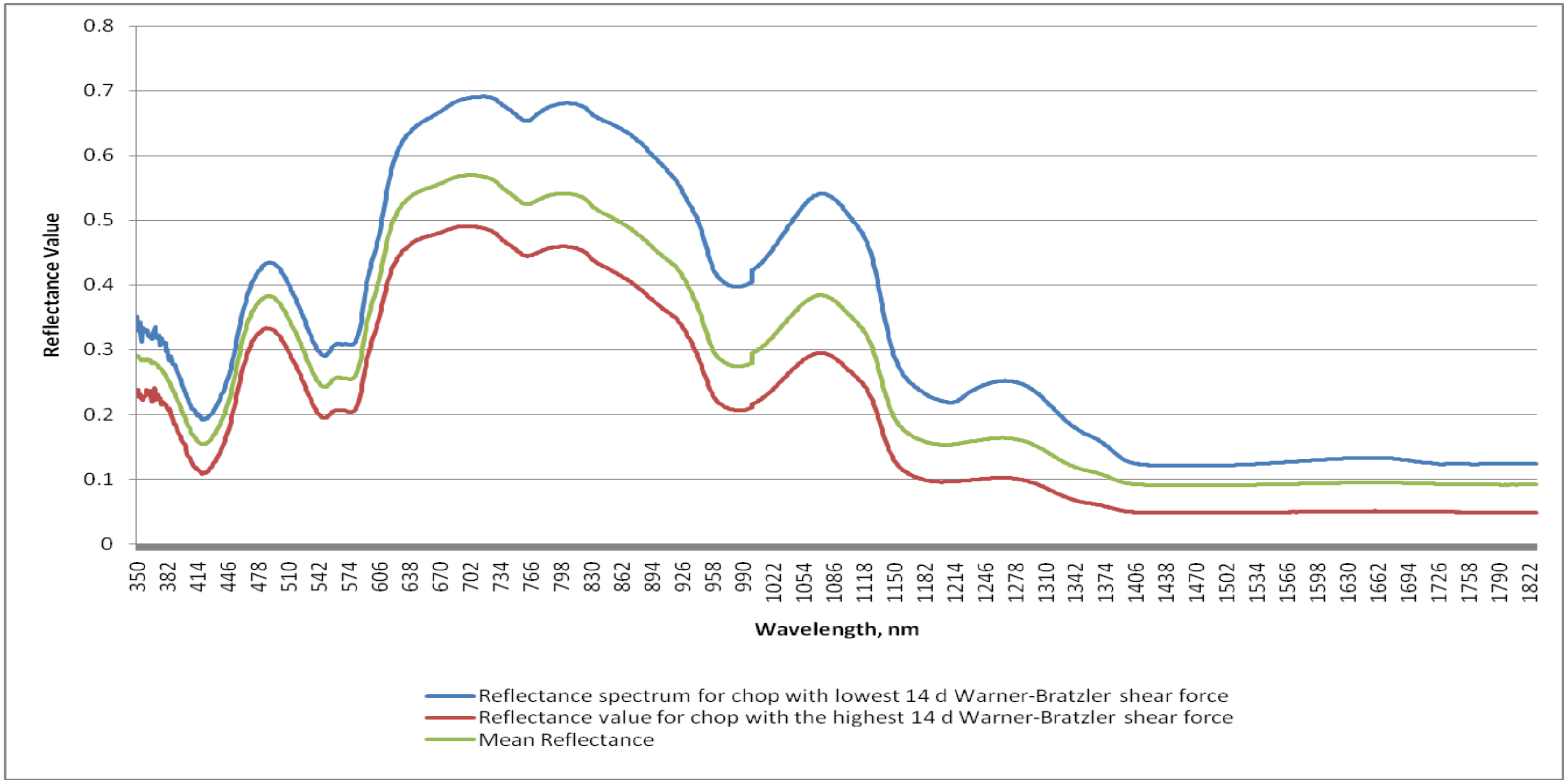

Figure 1 Mean reflectance values with spectrum from 350 nm to 1830 nm for the mean, and the toughest and most tender chop based on 13 day Warner-Bratzler shear force.

Have strong R^2 values. So VNIR wavelengths defined by Shackelford et al. (2005), 552-930 nm, were used in the PLSR equation for prediction of SSF and WBSF.

CHAPTER IV

RESULTS AND DISCUSSION

For the chop prediction data set, the *n*, means, standard deviation, minimum, and maximum values are presented in Table 1. All of the VNIR wavelengths and difference variables for the chop prediction data set are presented with the means, standard deviation, minimum, and maximum values in Table 1.

For the validation data set, the *n*, means, standard deviation, minimum, and maximum values are presented in Table 2, which were similar with all the above variables to the prediction data in Table 1.

Moeller et al. (2010) completed a study to view consumer pork eating quality as affected by pork quality attributes and the cooked end-point temperature. There were 679 fresh pork loin samples used in that study, the mean WBSF (N) at a cooked internal temperature of 62.8 °C was 24.6 N and for a cooked internal temperature of 68.3 °C, the mean WBSF was 25.9 N. The internal cooked temperature for our study was 65 °C and had a lower average WBSF (N) for the prediction and validation data sets than Moeller et al. (2010) found. Wright et al. (2005) also had a lower WBSF when their chops were cooked to an internal temperature of 70 °C. Wright et al. (2005) had a slightly lower L*color space values, and higher a* and b* color space values. pH values were fairly similar between this study and Moeller et al. (2010). Moeller et al. (2010) and Jeong et al. (2010) had a slightly higher average IMF % in their studies than reported in this study.

Table 1 Descriptive statistics for dependent and independent variables for the prediction data set where VNIR data were from the chop surface.

Variable	*n*	Mean	SD	Minimum	Maximum
Dependent Variables					
Slice Shear force, N	604	165.34	57.66	78.26	398.15
Warner-Bratzler Shear force, N	604	22.89	4.88	12.77	44.11
Lipid, %	604	2.21	0.94	0.37	6.11
Moisture %	604	74.07	0.97	70.37	77.49
Independent Variables					
pH	604	5.69	0.17	5.18	6.42
*L**	604	57.38	3.23	46.77	65.80
a*	604	4.80	0.65	3.26	7.34
b*	604	3.75	0.92	0.99	5.74
Resistance	604	42.42	4.94	29.70	60.20
Reactance	604	6.39	3.72	1.50	31.60
Phase Angle	604	8.22	3.74	1.50	30.50
Partial Capacitance	604	10431.12	3851.71	3457.60	44492.80
350 nm	604	0.29	0.05	0.12	0.46
373 nm	604	0.27	0.04	0.15	0.42
415 nm	604	0.14	0.03	0.08	0.29
485 nm	604	0.38	0.05	0.23	0.54
544 nm	604	0.24	0.04	0.13	0.39
624 nm	604	0.51	0.06	0.34	0.68
626 nm	604	0.51	0.06	0.35	0.69
698 nm	604	0.57	0.06	0.41	0.75
757 nm	604	0.53	0.05	0.37	0.71
799 nm	604	0.54	0.05	0.39	0.73
973 nm	604	0.28	0.04	0.18	0.43
1001 nm	604	0.30	0.04	0.18	0.50
1068 nm	604	0.39	0.05	0.25	0.60
1186 nm	604	0.16	0.03	0.07	0.34
1271 nm	604	0.16	0.03	0.08	0.34
1416 nm	604	0.09	0.03	0.03	0.26
1830 nm	604	0.09	0.02	0.03	0.26
Difference1[a]	604	0.11	0.02	0.04	0.18
Difference2[a]	604	-0.23	0.03	-0.30	-0.14
Difference3[a]	604	0.14	0.01	0.10	0.17
Difference4[a]	604	-0.27	0.03	-0.32	-0.18
Difference5[a]	604	-0.01	0.00	-0.00	-0.00
Difference6[a]	604	-0.06	0.01	-0.10	-0.03
Difference7[a]	604	0.04	0.01	0.02	0.06
Difference8[a]	604	-0.01	0.00	-0.03	-0.00
Difference9[a]	604	0.26	0.02	0.18	0.33
Difference10[a]	604	-0.02	0.01	-0.07	0.01
Difference11[a]	604	-0.09	0.01	-0.11	-0.06
Difference12[a]	604	0.23	0.03	0.15	0.30
Difference13[a]	604	-0.01	0.00	-0.02	-0.00
Difference14[a]	604	-0.07	0.02	0.04	0.14
Difference15[a]	604	-0.00	0.00	-0.01	0.01

[a] Difference 1= 373 nm – 415 nm; Difference 2 = 415 nm – 485 nm; Difference 3 = 485 nm – 544 nm; Difference 4 = 544 nm – 624; Difference 5= 624 nm -626 nm; Difference 6 = 626 nm – 698 nm; Difference 7 = 698 nm – 757 nm; Difference 8 = 757 nm – 799 nm; Difference 9 = 799 nm – 973 nm; Difference 10 = 973 nm – 1001 nm; Difference 11 = 1001 nm – 1068 nm; Difference 12 = 1068 nm – 1186 nm; Difference 13 = 1186 nm – 1271 nm; Difference 14 = 1271 nm – 1416 nm; and Difference 15 = 1416 nm – 1830 nm.

Table 2 Descriptive statistics for dependent and independent variables for the validation data set where VNIR data were from the chop surface.

Variable	*n*	Mean	SD	Minimum	Maximum
Dependent Variables					
Slice Shear Force, N	604	165.63	58.64	75.22	461.40
Warner-Bratzler Shear Force, N	604	23.01	5.43	12.52	59.70
Lipid, %	604	2.18	0.98	0.36	9.96
Moisture %	604	74.10	0.96	68.51	76.82
Independent Variables					
pH	604	5.71	0.18	5.31	6.56
*L**	604	56.90	3.46	45.44	66.04
a*	604	4.77	0.65	3.17	7.12
b*	604	3.62	0.96	0.75	6.61
Resistance	604	42.68	4.79	31.40	61.60
Reactance	604	6.46	3.81	1.40	29.10
Phase Angle	604	8.29	3.81	1.20	28.60
Partial Capacitance	604	10398.04	3618.35	3579.90	25302.00
350 nm	604	0.29	0.05	0.09	0.52
373 nm	604	0.27	0.05	0.12	0.48
415 nm	604	0.16	0.03	0.08	0.30
485 nm	604	0.38	0.05	0.25	0.60
544 nm	604	0.25	0.04	0.14	0.42
624 nm	604	0.51	0.06	0.35	0.74
626 nm	604	0.51	0.06	0.35	0.75
698 nm	604	0.57	0.06	0.41	0.80
757 nm	604	0.53	0.06	0.39	0.75
799 nm	604	0.54	0.06	0.40	0.77
973 nm	604	0.28	0.04	0.18	0.45
1001 nm	604	0.29	0.04	0.19	0.46
1068 nm	604	0.38	0.05	0.26	0.57
1186 nm	604	0.16	0.03	0.09	0.27
1271 nm	604	0.16	0.03	0.09	0.27
1416 nm	604	0.09	0.03	0.04	0.21
1830 nm	604	0.09	0.03	0.04	0.20
Difference1[a]	604	0.11	0.02	0.04	0.20
Difference2[a]	604	-0.22	0.03	-0.31	-0.14
Difference3[a]	604	0.14	0.01	0.10	0.17
Difference4[a]	604	-0.26	0.03	-0.35	0.19
Difference5[a]	604	-0.01	0.00	-0.01	-0.00
Difference6[a]	604	-0.05	0.01	-0.09	-0.03
Difference7[a]	604	0.04	0.01	0.02	0.06
Difference8[a]	604	-0.01	0.00	-0.03	-0.01
Difference9[a]	604	0.26	0.02	0.20	0.32
Difference10[a]	604	-0.02	0.01	-0.06	0.01
Difference11[a]	604	-0.09	0.01	-0.12	-0.06
Difference12[a]	604	0.23	0.03	0.15	0.34
Difference13[a]	604	0.01	0.00	-0.02	-0.00
Difference14[a]	604	0.07	0.02	0.03	0.15
Difference15[a]	604	-0.00	0.00	-0.01	0.01

[a] Difference 1= 373 nm – 415 nm; Difference 2 = 415 nm – 485 nm; Difference 3 = 485 nm – 544 nm; Difference 4 = 544 nm – 624; Difference 5= 624 nm -626 nm; Difference 6 = 626 nm – 698 nm; Difference 7 = 698 nm – 757 nm; Difference 8 = 757 nm – 799 nm; Difference 9 = 799 nm – 973 nm; Difference 10 = 973 nm – 1001 nm; Difference 11 = 1001 nm – 1068 nm; Difference 12 = 1068 nm – 1186 nm; Difference 13 = 1186 nm – 1271 nm; Difference 14 = 1271 nm – 1416 nm; and Difference 15 = 1416 nm – 1830 nm.

While slight differences existed in tenderness, pH, color and lipid, our data sets appear representative of pork carcasses found in the pork industry. Therefore, utilization of these data for the development of pork quality prediction equations should be applicable to the US pork industry.

The correlations between the dependent variables for the prediction data set are shown in Table 3. There was a positive relationship as expected between WBSF and SSF (r = 0.68). WBSF and SSF were similarly and negatively correlated to pH (-0.25 and -0.24). Chemical lipid and moisture were not highly related to WBSF (-0.18 and 0.03, respectively) and SSF (-0.09 and 0.06, respectively).

The simple correlation coefficients for the independent variables are shown in Table 4. The EI variables were highly correlated to each other and had low negative correlations to CIE L*, a*, b* color space values. The VNIR variables and difference variables were highly variable in range for correlation coefficients (r= -0.74 to 0.70) to EI variables and CIE L*, a* and b* color space values. CIE L*, a* and b* color space values are the reflectance values between 400- 700 nm (A.M.S.A., 1991), which contributes to the higher correlations to 415nm – 973 nm.

In Table 5, the simple correlation coefficients for the independent and dependent variables for the predicted chop data are shown. The EI variables had low positive relationships with WBSF, SSF, and pH. The CIE L*, a*, b* color space values were negatively correlated to pH (-0.52, -0.26, and -0.49, respectively), positively correlated to lipid (0.21, 0.13, and 0.20, respectively), and negatively correlated to moisture (-0.24,

Table 3 Simple correlation coefficients for dependent variables from the prediction data set.

Variable	*n*	pH	Lipid, %	Moisture, %	Warner-Bratzler Shear Force, N
Moisture, %	604				0.03
Lipid, %	604			-0.65[a]	-0.18[a]
pH	604		0.06	0.09 [a]	-0.25[a]
Slice Shear Force, N	604	-0.24[a]	-0.09[a]	-0.06	0.68[a]

[a]*P* –values greater than r = 0.08 are significant (P <0.05)

Table 4 Simple correlations coefficients between independent variables.

Variable	*n*	L*	a*	b*	Resistance	Reactance	Phase Angle	Partial Capacitance
Phase Angle	604							0.85[a]
Reactance	604						0.96[a]	0.81[a]
Resistance	604					0.77[a]	0.69[a]	0.45[a]
b*	604				-0.10[a]	-0.16[a]	-0.15[a]	-0.11[a]
a*	604			0.67[a]	-0.04[a]	-0.08[a]	-0.07	-0.05
L*	604		0.12[a]	0.71[a]	-0.06[a]	-0.14[a]	-0.12[a]	-0.12[a]
350 nm	604	0.42[a]	0.17[a]	0.38[a]	-0.12[a]	-0.15[a]	-0.14[a]	-0.13[a]
373 nm	604	0.52[a]	0.18[a]	0.45[a]	-0.13[a]	-0.17[a]	-0.16[a]	-0.17[a]
415 nm	604	0.30[a]	0.13[a]	0.30[a]	-0.08[a]	-0.13[a]	-0.14[a]	-0.14[a]
485 nm	604	0.66[a]	0.17[a]	0.54[a]	-0.13[a]	-0.18[a]	-0.17[a]	-0.13[a]
544 nm	604	0.65[a]	0.15[a]	0.54[a]	-0.11[a]	-0.17[a]	-0.17[a]	-0.14[a]
624 nm	604	0.70[a]	0.26[a]	0.62[a]	-0.14[a]	-0.23[a]	-0.21[a]	-0.18[a]
626 nm	604	0.70[a]	0.26[a]	0.62[a]	-0.14[a]	-0.23[a]	-0.21[a]	-0.18[a]
698 nm	604	0.67[a]	0.31[a]	0.62[a]	-0.14[a]	-0.23[a]	-0.23[a]	-0.20[a]
757 nm	604	0.66[a]	0.33[a]	0.62[a]	-0.12[a]	-0.23[a]	-0.23[a]	-0.21[a]
799 nm	604	0.63[a]	0.35[a]	0.61[a]	-0.11[a]	-0.23[a]	-0.23[a]	-0.21[a]
973 nm	604	0.54[a]	0.35[a]	0.55[a]	-0.05	-0.18[a]	-0.20[a]	-0.20[a]
1001 nm	604	0.50[a]	0.34[a]	0.53[a]	-0.04	-0.17[a]	-0.19[a]	-0.20[a]
1068 nm	604	0.54[a]	0.36[a]	0.56[a]	-0.04	-0.19[a]	-0.20[a]	-0.21[a]
1186 nm	604	0.28[a]	0.25[a]	0.35[a]	-0.01	-0.12[a]	-0.15[a]	-0.17[a]
1271 nm	604	0.30[a]	0.27[a]	0.37[a]	-0.00	-0.12[a]	-0.15[a]	-0.17[a]
1416 nm	604	-0.02	0.10[a]	0.07	-0.00	-0.05	-0.08[a]	-0.10[a]
1830 nm	604	-0.01	0.11[a]	0.09[a]	0.00	-0.05	-0.08[a]	-0.10[a]
Difference1[b]	604	0.62[a]	0.17[a]	0.50[a]	-0.14[a]	-0.17[a]	-0.14[a]	-0.10[a]
Difference2[b]	604	-0.74[a]	-0.13[a]	-0.56[a]	0.12[a]	0.16[a]	0.13[a]	0.08[a]
Difference3[b]	604	0.51[a]	0.16[a]	0.40[a]	-0.15[a]	-0.16[a]	-0.13[a]	-0.07
Difference4[b]	604	-0.64[a]	-0.36[a]	-0.60[a]	0.16[a]	0.25[a]	0.23[a]	0.20[a]
Difference5[b]	604	0.01	-0.30[a]	-0.14[a]	0.03	0.18[a]	0.20[a]	0.23[a]
Difference6[b]	604	0.19[a]	-0.34[a]	-0.03	-0.02	0.08[a]	0.11[a]	0.14[a]
Difference7[b]	604	0.48[a]	-0.03	0.31[a]	-0.23[a]	-0.19[a]	-0.14[a]	-0.07
Difference8[b]	604	0.33[a]	-0.26[a]	0.12[a]	-0.08[a]	-0.00	0.04	0.08[a]
Difference9[b]	604	0.65[a]	0.26[a]	0.56[a]	-0.19[a]	-0.25[a]	-0.22[a]	-0.17[a]
Difference10[b]	604	-0.08[a]	-0.10[a]	-0.12[a]	-0.06	0.01	0.04	0.08[a]
Difference11[b]	604	-0.62[a]	-0.39[a]	-0.60[a]	0.04	0.21[a]	0.22[a]	0.22[a]
Difference12[b]	604	0.68[a]	0.38[a]	0.65[a]	-0.06	-0.21[a]	-0.21[a]	-0.21[a]
Difference13[b]	604	-0.33[a]	-0.21[a]	-0.35[a]	-0.11[a]	0.06	0.08[a]	0.13[a]
Difference14[b]	604	0.62[a]	0.35[a]	0.59[a]	0.00	-0.15[a]	-0.16[a]	-0.17[a]
Difference15[b]	604	-0.22[a]	-0.08[a]	-0.17[a]	-0.07	-0.01	-0.00	0.02

[1]*P*-values greater than r = 0.08 are significant (*P* <0.05)

[2]Difference 1= 373 nm – 415 nm; Difference 2 = 415 nm – 485 nm; Difference 3 = 485 nm – 544 nm; Difference 4 = 544 nm – 624; Difference 5= 624 nm -626 nm; Difference 6 = 626 nm – 698 nm; Difference 7 = 698 nm – 757 nm; Difference 8 = 757 nm – 799 nm; Difference 9 = 799 nm – 973 nm; Difference 10 = 973 nm – 1001 nm; Difference 11 = 1001 nm – 1068 nm; Difference 12 = 1068 nm – 1186 nm; Difference 13 = 1186 nm – 1271 nm; Difference 14 = 1271 nm – 1416 nm; and Difference 15 = 1416 nm – 1830 nm.

Table 5 Simple Correlations coefficients for dependent and independent variables.

Variable	*n*	pH	Slice Shear Force, N	Lipid, %	Moisture, %	Warner-Bratzler Shear Force, N
Partial Capacitance	604	0.13[a]	0.16[a]	-0.11[a]	0.07	0.09[a]
Phase Angle	604	0.17[a]	0.19[a]	-0.05	0.02	0.10[a]
Reactance	604	0.20[a]	0.17[a]	-0.02	-0.01	0.08[a]
Resistance	604	0.18[a]	0.15[a]	0.16[a]	-0.15[a]	0.05
b*	604	-0.49[a]	0.03	0.20[a]	-0.26[a]	0.06
a*	604	-0.26[a]	0.04	0.13[a]	-0.19[a]	0.07
L*	604	-0.52[a]	0.07	0.21[a]	-0.24[a]	0.09[a]
350 nm	604	-0.35[a]	0.01	0.01	0.05	0.00
373 nm	604	-0.42[a]	-0.00	0.04	0.06	0.06
415 nm	604	-0.25[a]	-0.08[a]	0.09[a]	-0.04	-0.03
485 nm	604	-0.48[a]	0.02	0.10[a]	-0.11[a]	0.04
544 nm	604	-0.45[a]	-0.04	0.14[a]	-0.14[a]	-0.01
624 nm	604	-0.55[a]	0.00	0.15[a]	-0.16[a]	0.03
626 nm	604	-0.55[a]	0.01	0.15[a]	-0.16[a]	0.03
698 nm	604	-0.53[a]	-0.01	0.18[a]	-0.19[a]	0.01
757 nm	604	-0.52[a]	-0.03	0.22[a]	-0.22[a]	-0.01
799 nm	604	-0.51[a]	-0.04	0.24[a]	-0.23[a]	-0.02
973 nm	604	-0.40[a]	-0.12[a]	0.32[a]	-0.29[a]	-0.09[a]
1001 nm	604	-0.37[a]	-0.12[a]	0.31[a]	-0.27[a]	-0.10[a]
1068 nm	604	-0.39[a]	-0.11[a]	0.33[a]	-0.29[a]	-0.10[a]
1186 nm	604	-0.22[a]	-0.16[a]	0.24[a]	-0.20[a]	-0.12[a]
1271 nm	604	-0.21[a]	-0.17[a]	0.29[a]	-0.23[a]	-0.14[a]
1416 nm	604	-0.04	-0.14[a]	0.06	-0.03	-0.09[a]
1830 nm	604	-0.04	-0.15[a]	0.08[a]	-0.04	-0.09[a]
Difference1[b]	604	-0.50[a]	0.09[a]	-0.03	0.05	0.14[a]
Difference2[b]	604	0.51[a]	-0.11[a]	-0.07	0.14[a]	-0.09[a]
Difference3[b]	604	-0.45[a]	0.18[a]	-0.05	-0.01	0.18[a]
Difference4[b]	604	0.58[a]	-0.07	-0.14[a]	0.16[a]	-0.08[a]
Difference5[b]	604	0.05	0.03	-0.21[a]	0.17[a]	0.06
Difference6[b]	604	-0.05	0.11[a]	-0.24[a]	0.20[a]	0.13[a]
Difference7[b]	604	-0.45[a]	0.18[a]	-0.24[a]	0.15[a]	0.22[a]
Difference8[b]	604	-0.21[a]	0.13[a]	-0.29[a]	0.21[a]	0.17[a]
Difference9[b]	604	-0.57[a]	0.10[a]	0.04	-0.09[a]	0.10[a]
Difference10[b]	604	0.04	0.06	-0.09[a]	0.06	0.08[a]
Difference11[b]	604	0.41[a]	0.06	-0.37[a]	0.30[a]	0.08[a]
Difference12[b]	604	-0.48[a]	-0.03	0.34[a]	-0.31[a]	-0.06
Difference13[b]	604	0.03	0.18[a]	-0.62[a]	0.50[a]	0.25[a]
Difference14[b]	604	-0.35[a]	-0.10[a]	0.46[a]	-0.41[a]	-0.12[a]
Difference15[b]	604	0.00	-0.05	-0.27[a]	0.26[a]	0.05

[a]*P*-values greater than r = 0.08 are significant (*P* <0.05)

[b]Difference 1= 373 nm – 415 nm; Difference 2 = 415 nm – 485 nm; Difference 3 = 485 nm – 544 nm; Difference 4 = 544 nm – 624; Difference 5= 624 nm -626 nm; Difference 6 = 626 nm – 698 nm; Difference 7 = 698 nm – 757 nm; Difference 8 = 757 nm – 799 nm; Difference 9 = 799 nm – 973 nm; Difference 10 = 973 nm – 1001 nm; Difference 11 = 1001 nm – 1068 nm; Difference 12 = 1068 nm – 1186 nm; Difference 13 = 1186 nm – 1271 nm; Difference 14 = 1271 nm – 1416 nm; and Difference 15 = 1416 nm – 1830 nm.

Table 6 Simple correlation coefficients between VNIR reflectance values for peak, valley and difference VNIR data.

Variable	1830nm	1416nm	1271nm	1186nm	1068nm	1001nm	973nm	799nm	757nm	698nm	626nm	624nm	544nm	485nm	415nm	373nm	350nm
373nm																	0.97[a]
415nm																0.89[a]	0.85[a]
485nm															0.79[a]	0.91[a]	0.83[a]
544nm														0.98[a]	0.85[a]	0.90[a]	0.81[a]
624nm													0.94[a]	0.97[a]	0.72[a]	0.87[a]	0.78[a]
626nm												0.99[a]	0.94[a]	0.96[a]	0.72[a]	0.87[a]	0.78[a]
698nm											0.99[a]	0.99[a]	0.91[a]	0.93[a]	0.72[a]	0.85[a]	0.77[a]
757nm										0.99[a]	0.98[a]	0.98[a]	0.89[a]	0.91[a]	0.72[a]	0.84[a]	0.76[a]
799nm									0.99[a]	0.99[a]	0.96[a]	0.96[a]	0.87[a]	0.89[a]	0.72[a]	0.82[a]	0.75[a]
973nm								0.95[a]	0.93[a]	0.91[a]	0.87[a]	0.87[a]	0.83[a]	0.80[a]	0.79[a]	0.72[a]	0.79[a]
1001nm							0.99[a]	0.92[a]	0.91[a]	0.88[a]	0.84[a]	0.84[a]	0.81[a]	0.77[a]	0.78[a]	0.70[a]	0.76[a]
1068nm						0.99[a]	0.99[a]	0.94[a]	0.93[a]	0.90[a]	0.86[a]	0.85[a]	0.80[a]	0.77[a]	0.73[a]	0.75[a]	0.68[a]
1186nm					0.89[a]	0.93[a]	0.90[a]	0.75[a]	0.74[a]	0.70[a]	0.67[a]	0.66[a]	0.73[a]	0.65[a]	0.87[a]	0.71[a]	0.66[a]
1271nm				0.99[a]	0.99[a]	0.94[a]	0.91[a]	0.76[a]	0.75[a]	0.71[a]	0.67[a]	0.67[a]	0.73[a]	0.65[a]	0.85[a]	0.70[a]	0.65[a]
1416nm			0.86[a]	0.89[a]	0.89[a]	0.67[a]	0.62[a]	0.45[a]	0.44[a]	0.41[a]	0.39[a]	0.39[a]	0.54[a]	0.44[a]	0.84[a]	0.57[a]	0.55[a]
1830nm		0.99[a]	0.87[a]	0.90[a]	0.90[a]	0.69[a]	0.63[a]	0.46[a]	0.45[a]	0.42[a]	0.40[a]	0.40[a]	0.54[a]	0.45[a]	0.84[a]	0.58[a]	0.54[a]
Difference1[b]	0.08[a]	0.08[a]	0.32[a]	0.32[a]	0.55[a]	0.52[a]	0.55[a]	0.70[a]	0.72[a]	0.75[a]	0.78[a]	0.78[a]	0.70[a]	0.77[a]	0.49[a]	0.84[a]	0.82[a]
Difference2[b]	0.10[a]	0.11[a]	-0.21[a]	-0.19[a]	-0.51[a]	-0.46[a]	-0.50[a]	-0.70[a]	-0.73[a]	-0.77[a]	-0.82[a]	-0.82[a]	-0.73[a]	-0.81[a]	-0.29[a]	-0.58[a]	-0.48[a]
Difference3[b]	0.05	0.05	0.24[a]	0.24[a]	0.48[a]	0.44[a]	0.48[a]	0.69[a]	0.72[a]	0.76[a]	0.78[a]	0.78[a]	0.65[a]	0.80[a]	0.42[a]	0.68[a]	0.66[a]
Difference4[b]	-0.10[a]	-0.09[a]	-0.44[a]	-0.43[a]	-0.75[a]	-0.70[a]	-0.73[a]	-0.89	-0.89[a]	-0.90[a]	-0.88[a]	-0.88[a]	-0.66[a]	-0.74[a]	-0.40[a]	-0.64[a]	-0.58[a]
Difference5[b]	-0.20[a]	-0.10[a]	-0.33[a]	-0.32[a]	-0.43[a]	-0.40[a]	-0.41[a]	-0.41[a]	-0.37[a]	-0.33[a]	-0.22[a]	-0.21[a]	-0.06	-0.10[a]	-0.17[a]	-0.12[a]	-0.15[a]
Difference6[b]	-0.20[a]	-0.20[a]	-0.32[a]	-0.30[a]	-0.35[a]	-0.33[a]	-0.33[a]	-0.25[a]	-0.19[a]	-0.13[a]	0.01	0.02	0.18[a]	0.17[a]	-0.03	0.09[a]	0.04
Difference7[b]	-0.03	-0.02	0.03	0.05	0.20[a]	0.19[a]	0.22[a]	0.47[a]	0.52[a]	0.59[a]	0.66[a]	0.66[a]	0.61[a]	0.72[a]	0.35[a]	0.59[a]	0.53[a]
Difference8[b]	-0.19[a]	-0.18[a]	-0.24[a]	-0.22[a]	-0.18[a]	-0.17[a]	-0.16[a]	-0.02	0.05	0.12[a]	0.25[a]	0.25[a]	0.34[a]	0.37[a]	0.07	0.25[a]	0.19[a]
Difference9[b]	0.07	0.06	0.34[a]	0.34[a]	0.64[a]	0.59[a]	0.63[a]	0.85[a]	0.86[a]	0.89[a]	0.89[a]	0.89[a]	0.72[a]	0.82[a]	0.43[a]	0.67[a]	0.61[a]
Difference10[b]	-0.61[a]	-0.59[a]	-0.61[a]	-0.62[a]	-0.51[a]	-0.55[a]	-0.40[a]	-0.31[a]	-0.30[a]	-0.27[a]	-0.26[a]	-0.25[a]	-0.27[a]	-0.23[a]	-0.32[a]	-0.23[a]	-0.20[a]
Difference11[b]	-0.10[a]	-0.08[a]	-0.51[a]	-0.48[a]	-0.82[a]	-0.75[a]	-0.78[a]	-0.85[a]	-0.83[a]	-0.81[a]	-0.76[a]	-0.76[a]	-0.56[a]	-0.61[a]	-0.33[a]	-0.51[a]	-0.45[a]
Difference12[b]	0.12[a]	0.10[a]	0.55[a]	0.52[a]	0.86[a]	0.79[a]	0.82[a]	0.90[a]	0.89[a]	0.87[a]	0.84[a]	0.83[a]	0.66[a]	0.69[a]	0.38[a]	0.58[a]	0.52[a]
Difference13[b]	0.03	0.06	-0.37[a]	-0.30[a]	-0.50[a]	-0.46[a]	-0.48[a]	-0.38[a]	-0.35[a]	-0.31[a]	-0.27[a]	-0.27[a]	-0.21[a]	-0.17[a]	-0.04	-0.01	-0.06
Difference14[b]	0.08[a]	0.05	0.55[a]	0.50[a]	0.80[a]	0.75[a]	0.77[a]	0.76[a]	0.74[a]	0.71[a]	0.67[a]	0.67[a]	0.54[a]	0.54[a]	0.28[a]	0.44[a]	0.38[a]
Difference15[b]	0.46[a]	0.50[a]	0.16[a]	0.21[a]	-0.05	-0.00	0.04	0.00	0.01	0.02	0.03	0.03	0.18[a]	0.13[a]	0.49[a]	0.27[a]	0.28[a]

[a]*P*-values greater than r = 0.08 are significant (P <0.05)

[b]Difference 1= 373 nm – 415 nm; Difference 2 = 415 nm – 485 nm; Difference 3 = 485 nm – 544 nm; Difference 4 = 544 nm – 624; Difference 5= 624 nm -626 nm; Difference 6 = 626 nm – 698 nm; Difference 7 = 698 nm – 757 nm; Difference 8 = 757 nm – 799 nm; Difference 9 = 799 nm – 973 nm; Difference 10 = 973 nm – 1001 nm; Difference 11 = 1001 nm – 1068 nm; Difference 12 = 1068 nm – 1186 nm; Difference 13 = 1186 nm – 1271 nm; Difference 14 = 1271 nm – 1416 nm; and Difference 15 = 1416 nm – 1830 nm.

Table 7 Simple correlation coefficients between VNIR reflectance values for difference [b] data.

Variable	Difference2[b]	Difference3[b]	Difference4[b]	Difference5[b]	Difference6[b]	Difference7[b]	Difference8[b]	Difference9[b]	Difference10[b]	Difference11[b]	Difference12[b]	Difference13[b]	Difference14[b]	Difference15[b]
Difference14[b]														-0.52 [a]
Difference13[b]													-0.82 [a]	0.58 [a]
Difference12[b]												-0.59 [a]	0.91 [a]	-0.33 [a]
Difference11[b]											-0.98 [a]	0.59 [a]	-0.87 [a]	0.30 [a]
Difference10[b]										0.21 [a]	-0.25 [a]	0.15 [a]	-0.24 [a]	0.21 [a]
Difference9[b]									-0.08 [a]	-0.76 [a]	0.88 [a]	-0.12 [a]	0.55 [a]	-0.06
Difference8[b]								0.23 [a]	0.12 [a]	0.21 [a]	-0.10 [a]	0.31 [a]	-0.17 [a]	0.08 [a]
Difference7[b]							0.68 [a]	0.77 [a]	0.06	-0.23 [a]	0.32 [a]	0.27 [a]	0.08 [a]	0.13 [a]
Difference6[b]						0.46 [a]	0.91 [a]	-0.06	0.15 [a]	0.41 [a]	-0.32 [a]	0.28 [a]	-0.30 [a]	0.07
Difference5[b]					0.80 [a]	0.14 [a]	0.57 [a]	-0.30 [a]	0.13 [a]	0.50 [a]	-0.44 [a]	0.22 [a]	-0.34 [a]	0.02
Difference4[b]				0.38 [a]	0.21 [a]	-0.60 [a]	-0.08 [a]	-0.94 [a]	0.18 [a]	0.85 [a]	-0.90 [a]	0.30 [a]	-0.71 [a]	0.19 [a]
Difference3[b]			-0.80 [a]	-0.18 [a]	0.10 [a]	0.84 [a]	0.34 [a]	0.88 [a]	-0.05	-0.53 [a]	0.61 [a]	0.01	0.38 [a]	-0.04
Difference2[b]		-0.85 [a]	0.79 [a]	-0.00	-0.29 [a]	-0.79 [a]	-0.51 [a]	-0.87 [a]	0.05	0.64 [a]	-0.73 [a]	0.22 [a]	-0.58 [a]	0.26 [a]
Difference1[b]	-0.74[a]	0.78 [a]	-0.74 [a]	-0.03	0.19 [a]	0.69 [a]	0.39 [a]	0.70 [a]	-0.06	-0.57 [a]	0.65 [a]	-0.13 [a]	0.50 [a]	-0.07

[a]*P*-values greater than r = 0.08 are significant ($P < 0.05$)
[b]Difference 1= 373 nm – 415 nm; Difference 2 = 415 nm – 485 nm; Difference 3 = 485 nm – 544 nm; Difference 4 = 544 nm – 624; Difference 5= 624 nm -626 nm; Difference 6 = 626 nm – 698 nm; Difference 7 = 698 nm – 757 nm; Difference 8 = 757 nm – 799 nm; Difference 9 = 799 nm – 973 nm; Difference 10 = 973 nm – 1001 nm; Difference 11 = 1001 nm – 1068 nm; Difference 12 = 1068 nm – 1186 nm; Difference 13 = 1186 nm – 1271 nm; Difference 14 = 1271 nm – 1416 nm; and Difference 15 = 1416 nm – 1830 nm.

-0.19, and -0.26, respectively). VNIR and difference variables were more highly correlated similarly to CIE L* and b* color space values as correlations for individual variables used to calculate differences. The EI and VNIR variables were not highly related. Simple correlation coefficients for these VNIR variables for the prediction data sets are presented in Table 6 and Table 7. These VNIR values were highly correlated to each other. When wavelengths were close in the spectrum, difference variables tended to be more variable in relationships to individual reflectance values.

Shackelford et al. (1999a) reported a high correlation between SSF and WBSF (r = 0.80). The correlations in this study between percent lipid, percent moisture, pH, and tenderness were similar to that of Judge, Cahill, Kunkle & Deatherage (1960). Even though values were slightly different, Judge et al. (1960) reported higher correlations between tenderness and pH and higher correlations between pH and CIE L*, a*, and b* color space values, which were somewhat similar to that of Mancini & Hunt (2005). Nath (2008) reported higher correlations between EI variables (resistance, reactance, and phase angle) and WBSF (-0.12, 0.34, and 0.51, respectively) than this study, where correlations were much lower (0.05, 0.08, 0.10, respectively).

The stepwise regression formulas to predict pH, WBSF, SSF, moisture, and lipid are shown in Table 8. To predict these dependent variables using just the VNIR data, pH had moderate R^2 (0.47), SSF which was somewhat low (0.14), and WBSF which was also somewhat low (0.14). These R^2 values were slightly lower than that of Bowling et al. (2009), where they were able to have an R^2 value of 0.22 using similar but different wavelength values to predict WBSF in beef strip loin.

Stepwise regression formulas were developed using the pH and VNIR data as the independent variables (Table 9) to predict pH, WBSF, SSF, moisture, and lipid. With the addition of pH in the equation, the R^2 values increased slightly for WBSF ($R^2 = 0.17$), SSF ($R^2 = 0.20$), and moisture ($R^2 = 0.36$); however the R^2 value for the prediction of lipid remained the same ($R^2 = 0.43$). Thus by the addition of pH to VNIR wavelengths and difference variables, the prediction equation would have a higher ability to predict pork quality attributes.

Table 8 Stepwise regression using chop VNIR wavelengths and difference independent variables to predict pH, Warner-Bratzler shear force, Slice shear force, moisture, and lipid.

Dependent Variable	Intercept	β-Value	Independent Variable	Partial R^2	R^2
pH	6.09	1.29	350nm	0.01	0.47
		-3.83	373nm	0.01	
		3.17	757nm	0.01	
		-7.63	1068nm	0.01	
		7.96	1186nm	0.01	
		6.33	Difference 2[a]	0.01	
		12.65	Difference 3[a]	0.02	
		8.07	Difference 4[a]	0.34	
		21.40	Difference 8[a]	0.01	
		-26.30	Difference 11[a]	0.01	
		-13.41	Difference 13[a]	0.02	
		-31.59	Difference 15[a]	0.01	
Warner- Bratzler Shear Force, N	2.78	3.05	626nm	0.01	0.14
		-5.19	1416nm	0.01	
		10.29	Difference 3[a]	0.03	
		-10.18	Difference 4[a]	0.01	
		-19.13	Difference 9[a]	0.01	
		88.08	Difference 13[a]	0.06	
Slice Shear Force, N	13.15	-21.91	350nm	0.01	0.14
		250.30	626nm	0.01	
		-232.86	1068nm	0.01	
		159.15	Difference 2[a]	0.01	
		330.96	Difference 3[a]	0.03	
		-935.34	Difference 7[a]	0.01	
		-172.99	Difference 10[a]	0.01	
		306.54	Difference 13[a]	0.01	
Moisture, %	77.29	-4.35	626nm	0.04	0.31
		18.01	Difference 1[a]	0.01	
		-11.99	Difference 3[a]	0.01	
		205.16	Difference 13[a]	0.25	
Lipid, %	-1.17	16.58	415nm	0.02	0.43
		-13.09	973nm	0.01	
		-12.01	Difference 1[a]	0.01	
		-45.58	Difference 11[a]	0.01	
		-258.80	Difference 13[a]	0.38	

[a]Difference 1= 373 nm – 415 nm; Difference 2 = 415 nm – 485 nm; Difference 3 = 485 nm – 544 nm; Difference 4 = 544 nm – 624; Difference 5= 624 nm -626 nm; Difference 6 = 626 nm – 698 nm; Difference 7 = 698 nm – 757 nm; Difference 8 = 757 nm – 799 nm; Difference 9 = 799 nm – 973 nm; Difference 10 = 973 nm – 1001 nm; Difference 11 = 1001 nm – 1068 nm; Difference 12 = 1068 nm – 1186 nm; Difference 13 = 1186 nm – 1271 nm; Difference 14 = 1271 nm – 1416 nm; and Difference 15 = 1416 nm – 1830 nm.

Table 9 Stepwise regression using pH, chop VNIR wavelengths, and chop difference independent variables to predict Warner-Bratzler shear force, Slice shear force, moisture, and lipid.

Dependent Variable	Intercept	β-Value	Independent Variable	Partial R^2	R^2
Warner-Bratzler Shear Force, N	7.85	-0.87	pH	0.07	0.17
		0.65	350nm	0.01	
		-1.95	544nm	0.01	
		13.13	Difference 3[a]	0.00	
		-6.32	Difference 9[a]	0.01	
		55.06	Difference 13[a]	0.06	
		-36.30	Difference 15[a]	0.02	
Slice Shear Force, N	83.34	-11.59	pH	0.06	0.20
		-22.96	698nm	0.02	
		56.83	Difference 2[a]	0.01	
		210.46	Difference 3[a]	0.03	
		-3346.07	Difference 5[a]	0.00	
		499.78	Difference 6[a]	0.00	
		-667.25	Difference 8[a]	0.01	
		466.84	Difference 13[a]	0.00	
		-952.32	Difference 15[a]	0.01	
Moisture, %	72.72	0.71	pH	0.01	0.36
		10.44	350nm	0.00	
		-13.52	626nm	0.04	
		-38.05	973nm	0.01	
		23.34	1068nm	0.01	
		-32.23	Difference 3[a]	0.01	
		-5.07	Difference 4[a]	0.00	
		89.17	Difference 7[a]	0.00	
		287.67	Difference 13[a]	0.25	
		57.61	Difference 14[a]	0.01	
		183.67	Difference 15[a]	0.01	
Lipid, %	-1.17	16.58	415nm	0.02	0.43
		-13.09	973nm	0.01	
		-12.01	Difference 1[a]	0.01	
		-45.58	Difference 11[a]	0.01	
		-258.80	Difference 13[a]	0.38	

[a] Difference 1= 373 nm – 415 nm; Difference 2 = 415 nm – 485 nm; Difference 3 = 485 nm – 544 nm; Difference 4 = 544 nm – 624; Difference 5= 624 nm -626 nm; Difference 6 = 626 nm – 698 nm; Difference 7 = 698 nm – 757 nm; Difference 8 = 757 nm – 799 nm; Difference 9 = 799 nm – 973 nm; Difference 10 = 973 nm – 1001 nm; Difference 11 = 1001 nm – 1068 nm; Difference 12 = 1068 nm – 1186 nm; Difference 13 = 1186 nm – 1271 nm; Difference 14 = 1271 nm – 1416 nm; and Difference 15 = 1416 nm – 1830 nm.

When stepwise prediction equations were developed for dependent variables using pH and CIE L*, a* and b* color space values (Table 10), predictability was low. These data indicate that VNIR alone was a more acceptable technology to predict these dependent variables than using pH and CIE L*, a* and b* color space values.

When VNIR, pH, and CIE L*, a* and b* color space values were available as independent variables to predict pH, WBSF, SSF, moisture, and lipid, stepwise regression equations had the highest R^2 (Table 11). The two tenderness prediction equations include pH, color space values and VNIR values. While these two equations had higher R^2 than previous equations, R^2 values were low for WBSF and SSF (0.19 and 0.21, respectively).

Use of three technologies in combination did not account for a very high amount of variability in pork WBSF and SSF. Prediction equations for pH, moisture, and lipid included color space values in combination with VNIR data. These equations had slightly higher R^2, but the improvement in prediction was not appreciable.

A fourth technology was added to determine if prediction could be improved. Stepwise regression equations using the independent variables of pH, CIE L*, a* and b* color space values, and EI data are reported in Table 12. The addition of resistance in combination with L* and a* color space values improved the prediction of pork chop pH regression equations; however, addition of EI values to predict WBSF, SSF, moisture, and lipid resulted in lower R^2 values.

Table 10 Stepwise regression using pH and CIE L*, a* and b* color space values to predict pH, Warner-Bratzler shear force, Slice shear force, moisture, and lipid.

Dependent Variable	Intercept	β-Value	Independent Variable	Partial R^2	R^2
pH	7.52	-0.03	L*	0.27	0.31
		-0.05	a*	0.04	
Warner-Bratzler	7.07	-0.84	ph	0.06	0.07
Shear Force, N		0.07	b*	0.01	
		-0.08	a*	0.00	
Slice Shear	76.59	-9.99	pH	0.06	0.07
Force, N		-0.76	b*	0.01	
Moisture, %	83.02	-0.52	pH	0.01	0.09
		-0.08	L*	0.01	
		-0.28	a*	0.01	
Lipid, %	-12.82	1.47	pH	0.04	0.11
		-0.10	L*	0.04	
		0.24	a*	0.03	

Table 11 Stepwise regression using ph, CIE L* a* b*, chop VNIR wavelengths, and chop difference independent variables to predict pH, Warner-Bratzler shear force, Slice shear force, moisture, and lipid.

Dependent Variable	Intercept	β-Value	Independent Variable	Partial R^2	R^2
pH	6.80	-0.01	L*	0.04	0.49
		-0.03	a*	0.02	
		1.33	350nm	0.01	
		-3.31	Difference 1[a]	0.01	
		5.73	Difference 3[a]	0.02	
		3.68	Difference 4[a]	0.34	
		-5.84	Difference 6[a]	0.01	
		18.27	Difference 8[a]	0.01	
		-3.85	Difference 9[a]	0.01	
		-27.29	Difference 11[a]	0.04	
		-6.63	Difference 12[a]	0.01	
		-33.11	Difference 15[a]	0.00	
Warner-Bratzler Shear Force, N	4.09	-0.65	pH	0.07	0.19
		0.05	L*	0.00	
		0.16	a*	0.01	
		-0.01	b*	0.01	
		1.21	350nm	0.00	
		-3.70	544nm	0.00	
		7.14	Difference 3[a]	0.01	
		14.33	Difference 11[a]	0.01	
		38.88	Difference 13[a]	0.06	
		-20.99	Difference 15[a]	0.02	
Slice Shear Force, N	64.20	-10.70	pH	0.06	0.21
		0.26	L*	0.01	
		-25.05	350nm	0.01	
		140.01	Difference 2[a]	0.01	
		326.48	Difference 3[a]	0.03	
		-3337.30	Difference 5[a]	0.00	
		577.91	Difference 6[a]	0.00	
		-654.96	Difference 8[a]	0.01	
		416.50	Difference 13[a]	0.00	
		-970.81	Difference 15[a]	0.01	
Moisture, (%	81.43	-0.09	L*	0.02	0.38
		-0.14	a*	0.01	
		9.52	350nm	0.01	
		-16.68	799nm	0.01	
		-31.37	Difference 3[a]	0.01	
		74.39	Difference 7[a]	0.01	
		-53.98	Difference 11[a]	0.01	
		334.20	Difference 13[a]	0.25	
		44.92	Difference 14[a]	0.01	
Lipid, %	-3.68	0.51	L*	0.01	0.45
		11.81	415nm	0.02	
		-33.52	1271nm	0.01	
		27.61	1830nm	0.01	
		-10.66	Difference 1[a]	0.01	
		-20.74	Difference 8[a]	0.00	
		-31.23	Difference 11[a]	0.00	
		-319.89	Difference 13[a]	0.38	

[a] Difference 1= 373 nm – 415 nm; Difference 2 = 415 nm – 485 nm; Difference 3 = 485 nm – 544 nm; Difference 4 = 544 nm – 624; Difference 5= 624 nm -626 nm; Difference 6 = 626 nm – 698 nm; Difference 7 = 698 nm – 757 nm; Difference 8 = 757 nm – 799 nm; Difference 9 = 799 nm – 973 nm; Difference 10 = 973 nm – 1001 nm; Difference 11 = 1001 nm – 1068 nm; Difference 12 = 1068 nm – 1186 nm; Difference 13 = 1186 nm – 1271 nm; Difference 14 = 1271 nm – 1416 nm; and Difference 15 = 1416 nm – 1830 nm.

Table 12 Stepwise regression using ph, CIE L* a* and b* color space values, and electrical impedance independent variables to predict pH, Warner-Bratzler shear force, Slice shear force, moisture, and lipid.

Dependent Variable	Intercept	β-Value	Independent Variable	Partial R^2	R^2
pH	7.27	-0.03	L*	0.27	0.33
		-0.05	a*	0.04	
		0.01	Resistance	0.026	
Warner-Bratzler Shear Force, N	6.53	-0.77	pH	0.06	0.08
		0.02	Phase Angle	0.08	
Slice Shear Force, N	78.31	-10.90	pH	0.06	0.12
		-0.63	b*	0.01	
		0.36	Phase Angle	0.05	
Moisture, %	80.70	-0.07	L*	0.01	0.13
		-0.25	a*	0.01	
		-0.05	Resistance	0.03	
		0.00	Partial Capacitance	0.02	
Lipid, %	-13.34	1.29	pH	0.04	0.17
		0.09	L*	0.04	
		0.22	a*	0.03	
		0.06	Resistance	0.02	
		-0.07	Phase Angle	0.04	

Independent variables from four technologies, pH, CIE L*, a* and b* color space values, VNIR wavelengths, difference, and EI variables were used to predict pH, WBSF, SSF, moisture, and lipid (Table 13). These equations included variables from at least three to four of the technologies. The R^2 reported for these combined equations was the highest, especially for WBSF and SSF. However, predictability does not appear high enough to warrant use of three to four technologies.

VNIR Data Using the Rib Location

Location within the loin of where VNIR color assessments were taken has not been determined or examined. When pork loins are fabricated, assessment of tenderness using VNIR would be easier and faster if VNIR assessment was conducted on the medial edge of the loin instead of on the loin *M .longissimus* muscle surface. VNIR data were obtained from the medial aspect of the pork loin, defined as rib, and the *M. longissimus* muscle surface, defined as the chop. Prediction equations presented have only included chop VNIR values. To understand if loin location, chop or rib, would provide better prediction of dependent variables, additional equations were calculated using VNIR from the rib location.

Descriptive statistics for the predicted rib data are presented in Table 14. For the rib data, all the dependent variables and all the independent variables remain the same as the chop data, except for the location that VNIR data was acquired. The rib VNIR was very similar to data obtained from the chop. The means for all the variables only differ slightly from that of the chop with slightly higher standard deviation, and greater a range in general for minimum and maximum values. In Table 15 the descriptive statistics for

Table 13 Stepwise regression using EI, pH, CIE L*, a* and b* color space values, chop VNIR wavelengths, and chop difference independent variables to predict pH, Warner-Bratzler shear force, Slice shear force, moisture, and lipid.

Dependent Variable	Intercept	β-Value	Independent Variable	Partial R²	R²
Ph	6.79	-0.01	L*	0.34	0.49
		-0.03	a*	0.04	
		1.33	350nm	0.04	
		-3.32	Difference 1[a]	0.02	
		5.73	Difference 3[a]	0.01	
		3.68	Difference 4[a]	0.02	
		-5.83	Difference 6[a]	0.01	
		18.27	Difference 8[a]	0.00	
		-3.85	Difference 9[a]	0.01	
		-27.28	Difference 11[a]	0.01	
		-6.63	Difference 12[a]	0.01	
		-33.11	Difference 15[a]	0.01	
Warner-Bratzler	5.41	-0.68	pH	0.07	0.21
Shear Force, N		0.02	L*	0.01	
		0.06	a*	0.01	
		0.01	Resistance	0.02	
		14.09	Difference 3[a]	0.00	
		-6.49	Difference 4[a]	0.01	
		-15.72	Difference 9[a]	0.01	
		6.88	Difference 10[a]	0.01	
		87.92	Difference 13[a]	0.06	
		-49.11	Difference 15[a]	0.02	
Slice Shear Force, N	57.50	-11.46	pH	0.06	0.25
		0.23	L*	0.01	
		0.29	Resistance	0.05	
		-42.81	350nm	0.01	
		176.60	415nm	0.01	
		407.73	1186nm	0.01	
		-531.25	1271nm	0.01	
		119.13	Difference 2[a]	0.02	
		245.27	Difference 3[a]	0.04	
		-1934.68	Difference 15[a]	0.01	
Moisture, %	79.29	0.41	pH	0.01	0.39
		-0.08	L*	0.02	
		-0.13	a*	0.01	
		-0.02	Resistance	0.01	
		8.91	350nm	0.00	
		0.58	626nm	0.04	
		-16.46	799nm	0.01	
		1.07	Difference 1[a]	0.01	
		-30.02	Difference 3[a]	0.01	
		67.13	Difference 7[a]	0.01	
		-52.23	Difference 11[a]	0.01	
		336.61	Difference 13[a]	0.01	
		44.18	Difference 14[a]	0.01	
Lipid, %	-3.38	0.05	L*	0.01	0.45
		0.03	Resistance	0.01	
		-0.03	Phase Angle	0.01	
		13.98	415nm	0.02	
		-10.00	1186nm	0.01	
		-10.40	Difference 1[a]	0.01	
		-34.92	Difference 8[a]	0.01	
		-239.97	Difference 13[a]	0.38	

[a] Difference 1= 373 nm – 415 nm; Difference 2 = 415 nm – 485 nm; Difference 3 = 485 nm – 544 nm; Difference 4 = 544 nm – 624; Difference 5= 624 nm -626 nm; Difference 6 = 626 nm – 698 nm; Difference 7 = 698 nm – 757 nm; Difference 8 = 757 nm – 799 nm; Difference 9 = 799 nm – 973 nm; Difference 10 = 973 nm – 1001 nm; Difference 11 = 1001 nm – 1068 nm; Difference 12 = 1068 nm – 1186 nm; Difference 13 = 1186 nm – 1271 nm; Difference 14 = 1271 nm – 1416 nm; and Difference 15 = 1416 nm – 1830 nm.

Table 14 Descriptive statistics for VNIR wavelengths and difference independent variables for predicted rib data set.

Variable	*n*	Mean	SD	Minimum	Maximum
350 nm	604	0.26	0.05	0.04	0.50
373 nm	604	0.25	0.05	0.09	0.46
415 nm	604	0.14	0.03	0.06	0.33
485 nm	604	0.37	0.05	0.26	0.56
544 nm	604	0.23	0.04	0.15	0.42
624 nm	604	0.50	0.06	0.33	0.69
626 nm	604	0.50	0.06	0.34	0.70
698 nm	604	0.56	0.06	0.38	0.77
757 nm	604	0.52	0.06	0.36	0.72
799 nm	604	0.53	0.06	0.37	0.73
973 nm	604	0.27	0.04	0.17	0.43
1001 nm	604	0.29	0.04	0.18	0.47
1068 nm	604	0.38	0.05	0.24	0.56
1186 nm	604	0.15	0.03	0.08	0.31
1271 nm	604	0.15	0.03	0.09	0.31
1416 nm	604	0.08	0.03	0.03	0.25
1830 nm	604	0.08	0.03	0.03	0.24
Difference1[a]	604	0.11	0.02	0.03	0.17
Difference2 [a]	604	-0.24	0.03	-0.32	-0.15
Difference3 [a]	604	0.14	0.01	0.10	0.17
Difference4[a]	604	-0.26	0.07	-0.48	-0.08
Difference5 [a]	604	-0.01	0.00	-0.01	-0.00
Difference6 [a]	604	-0.06	0.01	-0.10	-0.03
Difference7 [a]	604	0.04	0.01	0.02	0.06
Difference8 [a]	604	-0.01	0.00	-0.04	-0.00
Difference9 [a]	604	0.26	0.02	0.18	0.32
Difference10[a]	604	-0.02	0.06	-0.23	0.16
Difference11[a]	604	-0.09	0.01	-0.12	-0.06
Difference12[a]	604	0.23	0.03	0.15	0.31
Difference13[a]	604	-0.01	0.00	-0.02	-0.00
Difference14[a]	604	-0.08	0.02	0.04	0.14
Difference15[a]	604	-0.00	0.00	-0.01	0.01

[a] Difference 1= 373 nm – 415 nm; Difference 2 = 415 nm – 485 nm; Difference 3 = 485 nm – 544 nm; Difference 4 = 544 nm – 624; Difference 5= 624 nm -626 nm; Difference 6 = 626 nm – 698 nm; Difference 7 = 698 nm – 757 nm; Difference 8 = 757 nm – 799 nm; Difference 9 = 799 nm – 973 nm; Difference 10 = 973 nm – 1001 nm; Difference 11 = 1001 nm – 1068 nm; Difference 12 = 1068 nm – 1186 nm; Difference 13 = 1186 nm – 1271 nm; Difference 14 = 1271 nm – 1416 nm; and Difference 15 = 1416 nm – 1830 nm.

Table 15 Descriptive statistics for VNIR wavelengths and difference independent variables for the validation rib data set.

Variable	*n*	Mean	SD	Minimum	Maximum
350 nm	604	0.26	0.06	0.09	0.46
373 nm	604	0.25	0.05	0.12	0.44
415 nm	604	0.14	0.04	0.07	0.30
485 nm	604	0.37	0.05	0.24	0.57
544 nm	604	0.23	0.04	0.14	0.40
624 nm	604	0.50	0.06	0.34	0.71
626 nm	604	0.50	0.06	0.35	0.71
698 nm	604	0.56	0.06	0.40	0.78
757 nm	604	0.52	0.06	0.37	0.72
799 nm	604	0.53	0.06	0.37	0.74
973 nm	604	0.27	0.04	0.18	0.45
1001 nm	604	0.29	0.05	0.17	0.59
1068 nm	604	0.38	0.06	0.24	0.68
1186 nm	604	0.15	0.04	0.07	0.42
1271 nm	604	0.15	0.04	0.08	0.42
1416 nm	604	0.08	0.03	0.03	0.33
1830 nm	604	0.08	0.03	0.03	0.33
Difference1[a]	604	0.11	0.02	0.01	0.17
Difference2[a]	604	-0.23	0.03	-0.31	-0.14
Difference3[a]	604	0.14	0.01	0.09	0.17
Difference4[a]	604	-0.27	0.07	-0.46	0.00
Difference5[a]	604	-0.01	0.00	-0.01	-0.00
Difference6[a]	604	-0.06	0.01	-0.09	-0.03
Difference7[a]	604	0.04	0.01	0.03	0.06
Difference8[a]	604	-0.01	0.00	-0.03	-0.00
Difference9[a]	604	0.26	0.02	0.19	0.31
Difference10[a]	604	-0.01	0.06	-0.34	0.19
Difference11[a]	604	-0.09	0.01	-0.12	-0.06
Difference12[a]	604	0.23	0.03	0.15	0.32
Difference13[a]	604	0.01	0.00	-0.02	-0.00
Difference14[a]	604	0.08	0.02	0.04	0.14
Difference15[a]	604	-0.00	0.00	-0.01	0.01

[a] Difference 1= 373 nm – 415 nm; Difference 2 = 415 nm – 485 nm; Difference 3 = 485 nm – 544 nm; Difference 4 = 544 nm – 624; Difference 5= 624 nm -626 nm; Difference 6 = 626 nm – 698 nm; Difference 7 = 698 nm – 757 nm; Difference 8 = 757 nm – 799 nm; Difference 9 = 799 nm – 973 nm; Difference 10 = 973 nm – 1001 nm; Difference 11 = 1001 nm – 1068 nm; Difference 12 = 1068 nm – 1186 nm; Difference 13 = 1186 nm – 1271 nm; Difference 14 = 1271 nm – 1416 nm; and Difference 15 = 1416 nm – 1830 nm.

the calibrated rib data are presented. The validation data set differ only slightly for all the variables in means, standard deviation, minimum, and maximum values from that of the prediction rib data set. These results indicate that this data set is also an acceptable representative of the quality attributes in the pork industry. Therefore, utilization of these data for development of pork quality prediction equations was acceptable.

Simple correlation coefficients for the VNIR variables from the rib for the prediction data sets are presented in Table 16, Table 17, Table 18, and Table 19. The correlation between independent and dependent variables for the rib data set (Table 16) were mostly slightly lower than that of the correlations of independent and dependent variables of the chop data set (Table 5). These VNIR wavelengths values were highly correlated to each other (r = 0.96 to 0.99), and some VNIR wavelengths were not highly related. For example, 973, 799, 757, 698, 626, and 624 nm were not highly correlated to 1001, 1068, 1186, 1271, 1416, and 1830 nm (r= 0.07 to 0.14). This indicates that reflectance values at different wavelengths may have been measuring different information. Simple correlation coefficients between VNIR rib difference variables tended to be lower than simple correlation coefficients between variables. However, simple correlation coefficients were similar to those reported for VNIR data from the chop surface. Based on the descriptive statistics and simple correlation data, VNIR data reflectance values taken on the rib loin surface had potential to be as good of a predictor of dependent variables as when VNIR reflectance values were obtained on the chop surface.

Table 16 Simple correlation coefficients for dependent and independent variables of the rib.

Variable	*n*	pH	Slice Shear Force, N	Lipid, %	Moisture, %	Warner-Bratzler Shear Force, N
350 nm	604	-0.18[a]	0.01	-0.01	0.11[a]	0.04
373 nm	604	-0.23[a]	-0.01	-0.00	0.08[a]	0.03
415 nm	604	-0.11[a]	0.02	-0.03	0.08[a]	0.03
485 nm	604	-0.33[a]	0.03	-0.09[a]	-0.04	0.03
544 nm	604	-0.29[a]	0.02	0.08[a]	-0.02	0.02
624 nm	604	0.06	-0.21[a]	0.03	0.05	-0.11[a]
626 nm	604	0.06	-0.21[a]	0.03	0.05	-0.11[a]
698 nm	604	0.07	-0.20[a]	0.02	0.06	-0.10[a]
757 nm	604	0.08[a]	-0.18[a]	0.02	0.07	-0.09[a]
799 nm	604	0.08[a]	-0.18[a]	0.02	0.07	-0.09[a]
973 nm	604	0.08[a]	-0.13[a]	0.03	0.08[a]	-0.07
1001 nm	604	-0.21[a]	-0.09[a]	0.27[a]	-0.19[a]	-0.07
1068 nm	604	-0.23[a]	-0.10[a]	0.31[a]	-0.23[a]	-0.08[a]
1186 nm	604	-0.09[a]	-0.09[a]	0.15[a]	0.09[a]	-0.06
1271 nm	604	-0.08[a]	-0.10[a]	0.19[a]	-0.12[a]	-0.07
1416 nm	604	0.03	-0.02	-0.05	0.06	-0.00
1830 nm	604	0.03	-0.03	-0.03	0.05	-0.01
Difference1[b]	604	-0.34[a]	-0.05	0.05	0.06	0.02
Difference2[b]	604	0.45[a]	-0.03	-0.19[a]	0.17[a]	-0.02
Difference3[b]	604	-0.34[a]	0.06[a]	0.09[a]	-0.09[a]	0.08[a]
Difference4[b]	604	-0.22[a]	0.19[a]	0.02	-0.06	0.10[a]
Difference5[b]	604	-0.11[a]	-0.01	0.06	-0.07	-0.04
Difference6[b]	604	-0.13[a]	0.01	0.04	-0.08[a]	-0.02
Difference7[b]	604	0.02	-0.26[a]	0.02	0.02	-0.13[a]
Difference8[b]	604	-0.11[a]	-0.10[a]	0.04	-0.05	-0.07
Difference9[b]	604	0.07	-0.22[a]	0.00	0.04	-0.09[a]
Difference10[b]	604	0.22[a]	-0.02	-0.18[a]	0.20[a]	0.00
Difference11[b]	604	0.29[a]	0.08[a]	-0.44[a]	0.35[a]	0.08[a]
Difference12[b]	604	-0.33[a]	-0.08[a]	0.42[a]	-0.33[a]	-0.08[a]
Difference13[b]	604	-0.02	0.12[a]	-0.57[a]	0.42[a]	0.18[a]
Difference14[b]	604	-0.23[a]	-0.15[a]	0.46[a]	-0.33[a]	-0.15[a]
Difference15[b]	604	-0.03	0.15[a]	-0.32[a]	0.22[a]	0.15[a]

[a]*P*-values greater than r = 0.08 are significant (*P* <0.05)

[b]Difference 1= 373 nm – 415 nm; Difference 2 = 415 nm – 485 nm; Difference 3 = 485 nm – 544 nm; Difference 4 = 544 nm – 624; Difference 5= 624 nm -626 nm; Difference 6 = 626 nm – 698 nm; Difference 7 = 698 nm – 757 nm; Difference 8 = 757 nm – 799 nm; Difference 9 = 799 nm – 973 nm; Difference 10 = 973 nm – 1001 nm; Difference 11 = 1001 nm – 1068 nm; Difference 12 = 1068 nm – 1186 nm; Difference 13 = 1186 nm – 1271 nm; Difference 14 = 1271 nm – 1416 nm; and Difference 15 = 1416 nm – 1830 nm.

Table 17 Simple Correlations Coefficients between independent variables for rib data set.

Variable	*n*	L*	a*	b*	Resistance	Reactance	Phase Angle	Partial Capacitance
350 nm	604	0.42[a]	0.17[a]	0.38[a]	-0.12[a]	-0.15[a]	-0.14[a]	-0.13[a]
373 nm	604	0.52[a]	0.18[a]	0.45[a]	-0.12[a]	-0.17[a]	-0.16[a]	-0.14[a]
415 nm	604	0.30[a]	0.14[a]	0.30[a]	-0.08[a]	-0.13[a]	-0.14[a]	-0.14[a]
485 nm	604	0.66[a]	0.17[a]	0.54[a]	-0.13[a]	-0.18[a]	-0.17[a]	-0.13[a]
544 nm	604	0.65[a]	0.15[a]	0.54[a]	-0.11[a]	-0.17[a]	-0.17[a]	-0.14[a]
624 nm	604	0.70[a]	0.26[a]	0.62[a]	-0.14[a]	-0.23[a]	-0.21[a]	-0.18[a]
626 nm	604	0.70[a]	0.26[a]	0.62[a]	-0.14[a]	-0.23[a]	-0.21[a]	-0.18[a]
698 nm	604	0.67[a]	0.31[a]	0.62[a]	-0.13[a]	-0.24[a]	-0.23[a]	-0.20[a]
757 nm	604	0.66[a]	0.33[a]	0.62[a]	-0.12[a]	-0.23[a]	-0.23[a]	-0.21[a]
799 nm	604	0.64[a]	0.35[a]	0.61[a]	-0.11[a]	-0.23[a]	-0.23[a]	-0.21[a]
973 nm	604	0.54[a]	0.35[a]	0.55[a]	-0.05	-0.19[a]	-0.20[a]	-0.20[a]
1001 nm	604	0.50[a]	0.34[a]	0.53[a]	-0.04	-0.17[a]	-0.19[a]	-0.20[a]
1068 nm	604	0.54[a]	0.36[a]	0.56[a]	-0.04	-0.19[a]	-0.20[a]	-0.21[a]
1186 nm	604	0.28[a]	0.25[a]	0.35[a]	-0.01	-0.12[a]	-0.15[a]	-0.16[a]
1271 nm	604	0.30[a]	0.26[a]	0.37[a]	-0.00	-0.12[a]	-0.15[a]	-0.17[a]
1416 nm	604	-0.02	0.10[a]	0.07	-0.00	-0.05	-0.08[a]	-0.10[a]
1830 nm	604	-0.01	0.11[a]	0.09[a]	0.00	-0.05	-0.08[a]	-0.10[a]
Difference1[b]	604	0.62[a]	0.17[a]	0.50[a]	-0.14[a]	-0.17[a]	-0.14[a]	-0.10[a]
Difference2[b]	604	-0.74[a]	-0.13[a]	-0.56[a]	0.12[a]	0.16[a]	0.13[a]	0.08[a]
Difference3[b]	604	0.51[a]	0.16[a]	0.40[a]	-0.15[a]	-0.16[a]	-0.13[a]	-0.07
Difference4[b]	604	-0.64[a]	-0.36[a]	-0.60[a]	0.16[a]	0.25[a]	0.24[a]	0.20[a]
Difference5[b]	604	0.00	-0.29[a]	-0.14[a]	0.03	0.18[a]	0.20[a]	0.23[a]
Difference6[b]	604	0.19[a]	-0.34[a]	-0.03	-0.02	0.08[a]	0.11[a]	0.14[a]
Difference7[b]	604	0.48[a]	-0.03	0.31[a]	-0.23[a]	-0.19[a]	-0.14[a]	-0.07
Difference8[b]	604	0.33[a]	-0.26[a]	0.11[a]	-0.08[a]	-0.00	0.04	0.08[a]
Difference9[b]	604	0.65[a]	0.26[a]	0.56[a]	-0.19[a]	-0.25[a]	-0.22[a]	-0.17[a]
Difference10[b]	604	-0.08[a]	-0.10[a]	-0.12[a]	-0.06	0.01	0.04	0.08[a]
Difference11[b]	604	-0.62[a]	-0.39[a]	-0.60[a]	0.04	0.21[a]	0.22[a]	0.22[a]
Difference12[b]	604	0.68[a]	0.38[a]	0.65[a]	-0.06	-0.21[a]	-0.21[a]	-0.21[a]
Difference13[b]	604	-0.33[a]	-0.21[a]	-0.34[a]	-0.11[a]	0.06	0.09[a]	0.13[a]
Difference14[b]	604	0.62[a]	0.35[a]	0.59[a]	0.00	-0.15[a]	-0.16[a]	-0.17[a]
Difference15[b]	604	-0.22[a]	-0.08[a]	-0.17[a]	-0.07	-0.01	-0.00	0.02

[a]*P*-values greater than r = 0.08 are significant (*P* <0.05)

[b] Difference 1= 373 nm – 415 nm; Difference 2 = 415 nm – 485 nm; Difference 3 = 485 nm – 544 nm; Difference 4 = 544 nm – 624; Difference 5= 624 nm -626 nm; Difference 6 = 626 nm – 698 nm; Difference 7 = 698 nm – 757 nm; Difference 8 = 757 nm – 799 nm; Difference 9 = 799 nm – 973 nm; Difference 10 = 973 nm – 1001 nm; Difference 11 = 1001 nm – 1068 nm; Difference 12 = 1068 nm – 1186 nm; Difference 13 = 1186 nm – 1271 nm; Difference 14 = 1271 nm – 1416 nm; and Difference 15 = 1416 nm – 1830 nm.

Table 18 Simple correlation coefficients prediction rib VNIR reflectance values for peak, valley and difference VNIR data.

Variable	1830nm	1416nm	1271nm	1186nm	1068nm	1001nm	973nm	799nm	757nm	698nm	626nm	624nm	544nm	485nm	415nm	373nm	350nm
373 nm																	0.97[a]
415 nm																0.92[a]	0.86[a]
485 nm															0.84[a]	0.89[a]	0.79[a]
544 nm														0.99[a]	0.89[a]	0.90[a]	0.80[a]
624 nm													0.06	0.05	0.08[a]	0.09[a]	0.09[a]
626 nm												0.99[a]	0.06	0.05	0.08[a]	0.09[a]	0.09[a]
698 nm											0.99[a]	0.99[a]	0.05	0.04	0.08[a]	0.09[a]	0.10[a]
757 nm										0.99[a]	0.98[a]	0.98[a]	0.05	0.04	0.07	0.09[a]	0.09[a]
799 nm									0.99[a]	0.99[a]	0.96[a]	0.96[a]	0.04	0.03	0.07	0.08[a]	0.09[a]
973 nm								0.96[a]	0.95[a]	0.93[a]	0.90[a]	0.90[a]	0.04	0.03	0.06	0.07	0.08[a]
1001 nm							0.08[a]	0.10[a]	0.11[a]	0.11[a]	0.13[a]	0.13[a]	0.80[a]	0.80[a]	0.73[a]	0.73[a]	0.65[a]
1068 nm						0.99[a]	0.07	0.09[a]	0.10[a]	0.10[a]	0.12[a]	0.12[a]	0.76[a]	0.78[a]	0.66[a]	0.68[a]	0.61[a]
1186 nm					0.89[a]	0.94[a]	0.10[a]	0.12[a]	0.12[a]	0.13[a]	0.14[a]	0.14[a]	0.80[a]	0.77[a]	0.85[a]	0.76[a]	0.68[a]
1271 nm				0.99[a]	0.91[a]	0.96[a]	0.10[a]	0.12[a]	0.12[a]	0.13[a]	0.14[a]	0.14[a]	0.79[a]	0.76[a]	0.83[a]	0.75[a]	0.67[a]
1416 nm			0.87[a]	0.90[a]	0.62[a]	0.71[a]	0.09[a]	0.10[a]	0.10[a]	0.11[a]	0.11[a]	0.11[a]	0.70[a]	0.64[a]	0.89[a]	0.71[a]	0.64[a]
1830 nm		0.99[a]	0.88[a]	0.91[a]	0.65[a]	0.73[a]	0.09[a]	0.11[a]	0.11[a]	0.11[a]	0.11[a]	0.11[a]	0.70[a]	0.64[a]	0.88[a]	0.71[a]	0.63[a]
Difference1[b]	0.19[a]	0.18[a]	0.37[a]	0.36[a]	0.49[a]	0.47[a]	0.06	0.07	0.08[a]	0.08[a]	0.09[a]	0.09[a]	0.61[a]	0.65[a]	0.48[a]	0.78[a]	0.81[a]
Difference2[b]	-0.07	-0.05	-0.35[a]	-0.33[a]	-0.58[a]	-0.53[a]	0.03	0.03	0.02	0.02	0.00	0.00	-0.67[a]	-0.76[a]	-0.27[a]	-0.45[a]	-0.35[a]
Difference3[b]	0.26[a]	0.25[a]	0.45[a]	0.44[a]	0.62[a]	0.59[a]	-0.01	-0.00	-0.00	-0.00	0.01	0.01	0.66[a]	0.78[a]	0.44[a]	0.59[a]	0.54[a]
Difference4[b]	0.31[a]	0.31[a]	0.35[a]	0.35[a]	0.35[a]	0.36[a]	-0.74[a]	-0.79[a]	-0.80[a]	-0.80[a]	-0.81[a]	-0.81[a]	0.53[a]	0.53[a]	0.45[a]	0.44[a]	0.40[a]
Difference5[b]	0.04	0.04	0.06	0.06	0.08[a]	0.08[a]	-0.40[a]	-0.43[a]	-0.39[a]	-0.36[a]	-0.24[a]	-0.24[a]	0.07	0.06	0.02	-0.00	-0.05
Difference6[b]	0.02	-0.02	0.02	0.01	0.06	0.05	-0.43[a]	-0.45[a]	-0.39[a]	-0.34[a]	-0.19[a]	-0.19[a]	0.05	0.05	-0.01	-0.01	-0.06
Difference7[b]	0.07	0.06	0.12[a]	0.12[a]	0.13[a]	0.13[a]	0.21[a]	0.38[a]	0.43[a]	0.50[a]	0.58[a]	0.58[a]	0.05	0.05	0.04	0.08[a]	0.08[a]
Difference8[b]	0.01	0.00	0.06	0.06	0.09[a]	0.09[a]	-0.29[a]	-0.22[a]	-0.16[a]	-0.09[a]	0.04	0.05	0.05	0.05	-0.01	0.01	-0.02
Difference9[b]	0.10[a]	0.10[a]	0.12[a]	0.12[a]	0.09[a]	0.10[a]	0.67[a]	0.85[a]	0.86[a]	0.87[a]	0.85[a]	0.85[a]	0.04	0.04	0.07	0.09[a]	0.09[a]
Difference10[b]	-0.49[a]	-0.48[a]	-0.66[a]	-0.64[a]	-0.70[a]	-0.70[a]	0.65[a]	0.61[a]	0.60[a]	0.58[a]	0.54[a]	0.55[a]	-0.58[a]	-0.59[a]	-0.51[a]	-0.50[a]	-0.44[a]
Difference11[b]	-0.05	-0.02	-0.43[a]	-0.39[a]	-0.75[a]	-0.65[a]	-0.00	-0.01	-0.01	-0.02	-0.04	-0.04	-0.36[a]	-0.43[a]	-0.13[a]	-0.27[a]	-0.24[a]
Difference12[b]	0.13[a]	0.09[a]	0.51[a]	0.49[a]	0.83[a]	0.75[a]	0.01	0.02	0.03	0.04	0.06	0.05	0.49[a]	0.56[a]	0.23[a]	0.38[a]	0.34[a]
Difference13[b]	0.11[a]	0.15[a]	-0.30[a]	-0.22[a]	-0.49[a]	-0.42[a]	-0.01	-0.01	-0.02	-0.02	-0.04	-0.04	-0.08[a]	-0.11[a]	0.08[a]	-0.01	0.00
Difference14[b]	0.08[a]	0.03	0.53[a]	0.47[a]	0.76[a]	0.70[a]	0.04	0.05	0.07	0.07	0.09[a]	0.09[a]	0.40[a]	0.44[a]	0.15[a]	0.29[a]	0.26[a]
Difference15[b]	0.40[a]	0.46[a]	0.08[a]	0.14[a]	-0.13[a]	-0.07	-0.00	-0.00	-0.01	-0.01	-0.03	-0.03	0.25[a]	0.19[a]	0.50[a]	0.32[a]	0.30[a]

[a]*P*-values greater than r = 0.08 are significant ($P < 0.05$)

[b] Difference 1= 373 nm – 415 nm; Difference 2 = 415 nm – 485 nm; Difference 3 = 485 nm – 544 nm; Difference 4 = 544 nm – 624; Difference 5= 624 nm -626 nm; Difference 6 = 626 nm – 698 nm; Difference 7 = 698 nm – 757 nm; Difference 8 = 757 nm – 799 nm; Difference 9 = 799 nm – 973 nm; Difference 10 = 973 nm – 1001 nm; Difference 11 = 1001 nm – 1068 nm; Difference 12 = 1068 nm – 1186 nm; Difference 13 = 1186 nm – 1271 nm; Difference 14 = 1271 nm – 1416 nm; and Difference 15 = 1416 nm – 1830 nm.

Table 19 Simple correlation coefficients rib difference [b] data.

Variable	Difference2[b]	Difference3[b]	Difference4[b]	Difference5[b]	Difference6[b]	Difference7	Difference8[b]	Difference9[b]	Difference10[b]	Difference11[b]	Difference12[b]	Difference13[b]	Difference14[b]	Difference15[b]
Difference15[b]														
Difference14[b]														-0.61[a]
Difference13[b]													-0.85[a]	0.64[a]
Difference12[b]												-0.68[a]	0.90[a]	-0.43[a]
Difference11[b]											-0.97[a]	0.67[a]	-0.83[a]	0.40[a]
Difference10[b]										0.50[a]	-0.56[a]	0.31[a]	-0.51[a]	0.06
Difference9[b]									0.40[a]	-0.02	0.04	-0.01	0.07	-0.00
Difference8[b]								-0.05	-0.28[a]	-0.10[a]	0.11[a]	-0.07	0.12[a]	-0.10[a]
Difference7[b]							0.66[a]	0.63[a]	0.05	-0.09[a]	0.11[a]	-0.07	0.14[a]	-0.10[a]
Difference6[b]						0.36[a]	0.88[a]	-0.38[a]	-0.35[a]	-0.09[a]	0.09[a]	-0.06	0.08[a]	-0.07
Difference5[b]					0.82[a]	0.20[a]	0.68[a]	-0.41[a]	-0.35[a]	-0.08[a]	0.08[a]	-0.05	0.06	-0.02
Difference4[b]				0.25[a]	0.19[a]	-0.47[a]	-0.01	-0.70[a]	-0.80[a]	-0.18[a]	0.24[a]	-0.02	0.16[a]	0.17[a]
Difference3[b]			0.38[a]	0.02	0.04	0.03	0.04	0.01	-0.46[a]	-0.58[a]	0.66[a]	-0.18[a]	0.47[a]	-0.06
Difference2[b]		-0.84[a]	-0.40[a]	-0.09[a]	-0.11[a]	-0.03	-0.10[a]	0.02	0.43[a]	0.62[a]	-0.71[a]	0.30[a]	-0.60[a]	0.25[a]
Difference1[b]	-0.58[a]	0.62[a]	0.29[a]	-0.04	-0.01	0.12[a]	0.04	0.08[a]	-0.32[a]	-0.40[a]	0.49[a]	-0.15[a]	0.43[a]	-0.07

[a]P-values greater than r = 0.08 are significant (P <0.05)
[b]Difference 1= 373 nm – 415 nm; Difference 2 = 415 nm – 485 nm; Difference 3 = 485 nm – 544 nm; Difference 4 = 544 nm – 624; Difference 5= 624 nm -626 nm; Difference 6 = 626 nm – 698 nm; Difference 7 = 698 nm – 757 nm; Difference 8 = 757 nm – 799 nm; Difference 9 = 799 nm – 973 nm; Difference 10 = 973 nm – 1001 nm; Difference 11 = 1001 nm – 1068 nm; Difference 12 = 1068 nm – 1186 nm; Difference 13 = 1186 nm – 1271 nm; Difference 14 = 1271 nm – 1416 nm; and Difference 15 = 1416 nm – 1830 nm.

Stepwise regression equations were developed and are shown in Table 20, these prediction equations were developed to predict pH, WBSF, SSF, moisture, and lipid using the rib data set with just the rib VNIR data. The prediction equation for all dependent variables was slightly lower than when VNIR data from the chop *M. longissimus* surface was used. Similar to that of the chop data set, R^2 values raised slightly with the addition of pH in the equations for the rib prediction stepwise regression equations shown in Table 21. When independent variables pH and VNIR were used in the prediction of WBSF, moisture, and lipid, as similarly reported in Table 18, the R^2 values were just slightly lower than those calculated using the VNIR values from the chop data set. For the SSF, however, the R^2 value numerically higher (R^2 = 0.23) than those reported using chop VNIR values (R^2 = 0.20).

In Table 22, stepwise regression prediction equations were developed using the dependent variables pH, CIE L*, a* and b* color space values, and rib VNIR to predict pH, WBSF, SSF, moisture, and lipid. The dependent variables had slightly lower R^2 values than those of equations developed from the chop data set. However, the R^2 value for predicting SSF (R^2 = 0.23) was slightly numerically higher using rib VNIR data than using chop VNIR data (R^2 = 0.21).

In Table 23, stepwise regression prediction equations were developed using the pH, CIE L*, a* and b* color space values, VNIR, and EI variables to predict pH, WBSF, SSF, moisture, and lipid. These prediction equations had slightly lower R^2 values than similar equations developed using VNIR values from the chop data set.

Table 20 Stepwise regression using rib VNIR wavelengths and difference independent variables to predict pH, Warner-Bratzler shear force, Slice shear force, moisture, and lipid.

Dependent Variable	Intercept	β-Value	Independent Variable	Partial R^2	R^2
pH	5.73	2.39	485nm	0.01	0.38
		-9.54	1001nm	0.02	
		3.95	1068nm	0.01	
		-39.14	1416nm	0.03	
		44.76	1830nm	0.01	
		-2.07	Difference 1[a]	0.01	
		4.50	Difference 2[a]	0.20	
		4.30	Difference 3[a]	0.03	
		-4.57	Difference 6[a]	0.01	
		8.54	Difference 7[a]	0.01	
		-1.24	Difference 9[a]	0.00	
		-30.32	Difference 13[a]	0.03	
Warner-Bratzler Shear Force, N	2.33	5.48	Difference 3[a]	0.01	0.06
		-11.94	Difference 7[a]	0.02	
		36.78	Difference 13[a]	0.03	
Slice Shear Force, N	26.68	-22.28	1271nm	0.01	0.12
		65.74	Difference 3[a]	0.00	
		-1104.64	Difference 5[a]	0.01	
		129.79	Difference 6[a]	0.01	
		-324.00	Difference 7[a]	0.07	
		477.44	Difference 15[a]	0.02	
Moisture, %	76.58	10.15	Difference 1[a]	0.02	0.24
		-56.64	Difference 11[a]	0.01	
		-44.66	Difference 12[a]	0.02	
		236.58	Difference 13[a]	0.18	
		44.04	Difference 14[a]	0.02	
Lipid, %	-0.22	-3.14	373nm	0.01	0.36
		6.52	544nm	0.01	
		-8.75	Difference 3[a]	0.00	
		-31.87	Difference 11[a]	0.01	
		-258.68	Difference 13[a]	0.33	
		-23.66	Difference 14[a]	0.02	

[a] Difference 1= 373 nm – 415 nm; Difference 2 = 415 nm – 485 nm; Difference 3 = 485 nm – 544 nm; Difference 4 = 544 nm – 624; Difference 5= 624 nm -626 nm; Difference 6 = 626 nm – 698 nm; Difference 7 = 698 nm – 757 nm; Difference 8 = 757 nm – 799 nm; Difference 9 = 799 nm – 973 nm; Difference 10 = 973 nm – 1001 nm; Difference 11 = 1001 nm – 1068 nm; Difference 12 = 1068 nm – 1186 nm; Difference 13 = 1186 nm – 1271 nm; Difference 14 = 1271 nm – 1416 nm; and Difference 15 = 1416 nm – 1830 nm.

Table 21 Stepwise regression using pH, rib VNIR wavelengths, and rib difference independent variables to predict Warner-Bratzler shear force, Slice shear force, moisture, and lipid.

Dependent Variable	Intercept	β-Value	Independent Variable	Partial R^2	R^2
Warner-Bratzler Shear Force, N	7.18	-0.82	pH	0.06	0.13
		3.36	Difference 2[a]	0.01	
		10.51	Difference 3[a]	0.01	
		-9.72	Difference 7[a]	0.01	
		-5.96	Difference 14[a]	0.04	
Slice Shear Force, N	91.47	-11.09	pH	0.06	0.23
		71.83	350nm	0.01	
		239.76	1001nm	0.00	
		-666.14	1416nm	0.01	
		368.37	1830nm	0.01	
		-171.70	Difference 1[a]	0.00	
		39.69	Difference 3[a]	0.02	
		-1019.47	Difference 5[a]	0.00	
		94.74	Difference 6[a]	0.00	
		-251.59	Difference 7[a]	0.07	
		202.87	Difference 11[a]	0.01	
		-1047.49	Difference 13[a]	0.01	
		-560.69	Difference 14[a]	0.03	
Moisture, %	71.93	0.74	pH	0.02	0.26
		10.75	Difference 1[a]	0.02	
		-53.03	Difference 11[a]	0.01	
		-41.19	Difference 12[a]	0.02	
		261.95	Difference 13[a]	0.18	
		45.61	Difference 14[a]	0.02	
Lipid, %	-0.75	-3.28	373nm	0.01	0.36
		5.59	544nm	0.01	
		-26.52	Difference 11[a]	0.01	
		-271.42	Difference 13[a]	0.33	
		-24.67	Difference 14[a]	0.02	

[a] Difference 1= 373 nm – 415 nm; Difference 2 = 415 nm – 485 nm; Difference 3 = 485 nm – 544 nm; Difference 4 = 544 nm – 624; Difference 5= 624 nm -626 nm; Difference 6 = 626 nm – 698 nm; Difference 7 = 698 nm – 757 nm; Difference 8 = 757 nm – 799 nm; Difference 9 = 799 nm – 973 nm; Difference 10 = 973 nm – 1001 nm; Difference 11 = 1001 nm – 1068 nm; Difference 12 = 1068 nm – 1186 nm; Difference 13 = 1186 nm – 1271 nm; Difference 14 = 1271 nm – 1416 nm; and Difference 15 = 1416 nm – 1830 nm.

Table 22 Stepwise regression using ph, CIE L* a* b*, rib VNIR wavelengths, and rib difference independent variables to predict pH, Warner-Bratzler shear force, Slice shear force, moisture, and lipid.

Dependent Variable	Intercept	β-Value	Independent Variable	Partial R^2	R^2
pH	7.13	-0.02	L*	0.27	0.44
		-0.05	a*	0.04	
		-21.25	1416nm	0.02	
		22.92	1830nm	0.01	
		-1.74	Difference 6[a]	0.01	
		-17.47	Difference 11[a]	0.02	
		-8.95	Difference 12[a]	0.01	
		-21.76	Difference 13[a]	0.03	
Warner-Bratzler Shear Force, N	7.18	-0.82	pH	0.06	0.13
		3.36	Difference 2[a]	0.01	
		10.51	Difference 3[a]	0.01	
		-9.72	Difference 7[a]	0.01	
		-5.95	Difference 14[a]	0.04	
Slice Shear Force, N	91.47	-11.09	pH	0.06	0.23
		71.83	350nm	0.01	
		239.76	1001nm	0.00	
		-666.14	1416nm	0.01	
		368.37	1830nm	0.01	
		-171.70	Difference 1[a]	0.00	
		39.69	Difference 3[a]	0.01	
		-1091.47	Difference 5[a]	0.00	
		94.74	Difference 6[a]	0.00	
		-251.59	Difference 7[a]	0.07	
		202.87	Difference 11[a]	0.01	
		-1047.49	Difference 13[a]	0.01	
		-560.69	Difference 14[a]	0.03	
Moisture, %	78.36	-0.05	L*	0.01	0.30
		-0.17	b*	0.03	
		11.84	Difference 1[a]	0.03	
		1.29	Difference 10[a]	0.01	
		-65.72	Difference 11[a]	0.01	
		-44.77	Difference 12[a]	0.02	
		292.91	Difference 13[a]	0.18	
		56.52	Difference 14[a]	0.01	
Lipid, %	-7.37	0.65	pH	0.01	0.38
		0.07	L*	0.01	
		2.76	1001nm	0.01	
		-22.73	Difference 11[a]	0.01	
		-277.35	Difference 13[a]	0.33	
		-29.31	Difference 14	0.02	

[a] Difference 1= 373 nm – 415 nm; Difference 2 = 415 nm – 485 nm; Difference 3 = 485 nm – 544 nm; Difference 4 = 544 nm – 624; Difference 5= 624 nm -626 nm; Difference 6 = 626 nm – 698 nm; Difference 7 = 698 nm – 757 nm; Difference 8 = 757 nm – 799 nm; Difference 9 = 799 nm – 973 nm; Difference 10 = 973 nm – 1001 nm; Difference 11 = 1001 nm – 1068 nm; Difference 12 = 1068 nm – 1186 nm; Difference 13 = 1186 nm – 1271 nm; Difference 14 = 1271 nm – 1416 nm; and Difference 15 = 1416 nm – 1830 nm.

Table 23 Stepwise regression using pH, CIE L*, a* and b* color space values, EI, rib VNIR wavelengths, and rib difference independent variables to predict pH, Warner-Bratzler shear force, Slice shear force, moisture, and lipid.

Dependent Variable	Intercept	β-Value	Independent Variable	Partial R²	R²
pH	6.87	-0.02	L*	0.27	0.45
		-0.05	a*	0.04	
		0.00	Resistance	0.01	
		-19.92	1416nm	0.02	
		21.46	1830nm	0.01	
		-2.31	Difference 6[a]	0.01	
		2.79	Difference 7[a]	0.01	
		-15.94	Difference 11[a]	0.01	
		-8.37	Difference 12[a]	0.01	
		-20.61	Difference 13[a]	0.03	
Warner-Bratzler Shear Force, N	7.09	-0.85	pH	0.06	0.14
		0.02	Phase Angle	0.01	
		3.24	Difference 2[a]	0.01	
		10.81	Difference 3[a]	0.01	
		-8.01	Difference 7[a]	0.01	
		-5.75	Difference 14[a]	0.04	
Slice Shear Force, N	78.01	-11.16	pH	0.06	0.21
		0.15	Resistance	0.01	
		0.13	Phase Angle	0.04	
		89.12	Difference 3[a]	0.01	
		-199.83	Difference 7[a]	0.07	
		-615.97	Difference 13[a]	0.01	
		-177.75	Difference 14[a]	0.02	
Moisture, %	79.06	-0.06	L*	0.01	0.31
		-0.17	b*	0.03	
		8.80	Difference 1[a]	0.03	
		5.06	Difference 4[a]	0.01	
		23.10	Difference 7[a]	0.01	
		6.73	Difference 10[a]	0.01	
		-72.55	Difference 11[a]	0.01	
		-45.44	Difference 12[a]	0.02	
		308.59	Difference 13[a]	0.18	
		64.71	Difference 14[a]	0.01	
Lipid, %	-7.71	0.70	pH	0.01	0.39
		0.05	L*	0.01	
		0.01	Resistance	0.01	
		-0.00	Partial Capacitance	0.01	
		12.31	Difference 12[a]	0.02	
		-268.27	Difference 13[a]	0.33	
		-31.24	Difference 14[a]	0.01	

[a] Difference 1= 373 nm – 415 nm; Difference 2 = 415 nm – 485 nm; Difference 3 = 485 nm – 544 nm; Difference 4 = 544 nm – 624; Difference 5= 624 nm -626 nm; Difference 6 = 626 nm – 698 nm; Difference 7 = 698 nm – 757 nm; Difference 8 = 757 nm – 799 nm; Difference 9 = 799 nm – 973 nm; Difference 10 = 973 nm – 1001 nm; Difference 11 = 1001 nm – 1068 nm; Difference 12 = 1068 nm – 1186 nm; Difference 13 = 1186 nm – 1271 nm; Difference 14 = 1271 nm – 1416 nm; and Difference 15 = 1416 nm – 1830 nm.

Similar to that of the chop data set, the rib data set prediction equations for pH, WBSF, SSF, moisture, and lipid were highest when all the independent variables (VNIR, pH, Color, and EI) are used. However, in a practical on-line usage, the prediction equation using just three variables (VNIR, pH, and color) could be sufficient in providing similar predictability as equations using four technologies. In concurrent with Moeller et al. (2010), pH played a major role in the prediction equations for WBSF and SSF. Whether in consumer perceptions (Moeller et al., 2010) or objective measured, pH played a large role in each prediction equation. Judge et al. (1960) also used pH in a regression equation for the prediction of tenderness; however, pH accounted for a higher amount of variability for predicting tenderness than in our study. Wulf & Page (2000), reported that L* color space values and pH both played roles in predicting beef palatability.

When comparing the rib and chop data set, using VNIR data from the chop data set had similar if not stronger predictability than prediction equations developed using VNIR values from the rib. The greatest disadvantage for using equations for VNIR chop lean surface evaluation is that the pork carcasses would have to be ribbed. Pork carcasses are not normally ribbed in pork harvest plants. Industry would most likely use VNIR rib equation if they utilize VNIR to predict pork tenderness.

Partial Least Squares Regression

Stepwise linear regression equations, regardless of technology, were not highly predictive. Use of Partial Least Squares Regression (PLSR) is a multivariate statistical method that removes auto correlations between independent variables. Three strategies were used to develop PLSR equations. First, models that include the predetermined peaks, valleys, and differences in wavelengths for chop VNIR data were used in combination with pH, CIE L*, a* and b* color space values, and EI data to predict WBSF and SSF. These models were not highly predictive. A second model was evaluated that utilized all VNIR chop wavelengths from 350 nm to 1830 nm in combination with the other independent variables. This model also was not highly predictive. Shackelford et al. (2005) converted SSF data from continuous to categorical data, and were able to have a higher percentage of tenderness predictability.

PLSR were developed and shown in Table 23 and Table 24 for the chop data set, which comprised of the reflectance values from wavelengths between 552 – 930nm. The data set was divided into categories of “tough” (WBSF >34.3 N), “intermediate” (WBSF >24.5 N, WBSF < 34.3 N), and “tender” (WBSF < 24.5 N). By using PLSR, with an R^2 value of 0.49, 100 % of the “tender” chops were correctly classified, 93 % of the “intermediate” chops were correctly classified, and 92% of the “tough” chops were correctly classified into its category for WBSF. However, for SSF was much lower (R^2 = 0.24) with only correctly placing 62 % of the “tender” chops and only 48 % of the “intermediate” and “tough” chops.

Table 24 Partial least squares regression chop data with VNIR data 552-930nm wavelengths for Warner-Bratzler shear force and Slice shear force.

Category	Actual	Predicted	Incorrectly Predicted	% Correctly Classified	R^2
WBSF					
Tender*	415	429	14	100 %	0.49
Intermediate*	164	152	16	93 %	0.49
Tough*	25	23	0	92 %	0.49
SSF					
Tender**	291	290	109	62 %	0.24
Intermediate**	248	248	129	48 %	0.24
Tough**	65	66	35	48 %	0.24

*"Tender" was defined to have a WBSF <24.5 N
*"Intermediate" was defined to a WBSF >24.5 but <34.3 N
*"Tough" was defined to have a WBSF >34.3 N
**"Tender" was defined to have a SSF < 147.1 N
**"Intermediate" was defined to have a SSF >147.1 but <245.2 N
**"Tough" was defined to have a SSF >245.2 N

CHAPTER V

CONCLUSION

In conclusion, it is apparent that VNIR, pH, and color played the greatest roles in predicting tenderness of pork. However, in an on-line situation similar to that of industry, with as weakly as the independent variables were able to predict the different pork quality attributes, possibly more work needs to be done on these methods. VNIR reflectance values show a high ability to predict WBSF on the chop surface; therefore, could be applicable in a situation where this is available.

REFERENCES

A.M.S.A. (1991). Guidelines for Meat Color Evaluation. In *Proceedings of the Reciprocal Meat Conference,* Savoy, IL.

AOAC (1995). *Official methods of analysis* (16th ed.). Arlington, VA: Association of Official Analytical Chemists.

Barbosa-Silva, M. C. G., & Barros, A. J. D. (2005). Bioelectrical impedance analysis in clinical practice: A new perspective on its use beyond body composition equations. *Current Opinion in Clinical Nutrition & Metabolic Care*, *8*, 311-317.

Bouton, P. E., Harris, P. V., & Shorthose, W. R. (1971). Effect of ultimate pH upon the water-holding capacity and tenderness of mutton. *Journal of Food Science*, *36*, 435-439.

Bowling, M. B., Vote, D. J., Belk, K. E., Scanga, J. A., Tatum, J. D., & Smith, G. C. (2009). Using reflectance spectroscopy to predict beef tenderness. *Meat Science*, *82*, 1-5.

Brewer, M., Jensen, J., Prestat, C., Zhu, L., & McKeith, F. (2002). Visual acceptability and consumer purchase intent of enhanced pork loin roasts. *Journal of Muscle Foods*, *13*, 53-68.

Brosnan, T., & Sun, D.-W. (2002). Inspection and grading of agricultural and food products by computer vision systems--a review. *Computers and Electronics in Agriculture*, *36*, 193-213.

Cameron, N. D. (1990). Genetic and phenotypic parameters for carcass traits, meat and eating quality traits in pigs. *Livestock Production Science*, *26*, 119-135.

Davis, G. W., Smith, G. C., Carpenter, Z. L., & Cross, H. R. (1975). Relationships of quality indicators to palatability attributes of pork loins. *Journal of Animal Science*, *41*, 1305-1313.

DeVol, D. L., McKeith, F. K., Bechtel, P. J., Novakofski, J., Shanks, R. D., & Carr, T. R. (1988). Variation in composition and palatability traits and relationships between muscle characteristics and palatability in a random sample of pork carcasses. *Journal of Animal Science*, *66*, 385-395.

Gault, N. F. S. (1985). The relationship between water-holding capacity and cooked meat tenderness in some beef muscles as influenced by acidic conditions below the ultimate pH. *Meat Science*, *15*, 15-30.

Hoving-Bolink, A. H., Vedder, H. W., Merks, J. W. M., de Klein, W. J. H., Reimert, H. G. M., Frankhuizen, R., van den Broek, W. H. A. M., & Lambooij, e. E. (2005). Perspective of NIRS measurements early post mortem for prediction of pork quality. *Meat Science*, *69*, 417-423.

Jeong, D. W., Choi, Y. M., Lee, S. H., Choe, J. H., Hong, K. C., Park, H. C., & Kim, B. C. (2010). Correlations of trained panel sensory values of cooked pork with fatty acid composition, muscle fiber type, and pork quality characteristics in Berkshire pigs. *Meat Science*, *86*, 607-615.

Jeremiah, L. E., & Gibson, L. L. (1991). The usefulness of muscle color and pH for segregating beef carcasses into tenderness groups. *Meat Science*, *30*, 97-114.

Judge, M. D., Cahill, V. R., Kunkle, L. E., & Deatherage, F. E. (1960). Pork quality II. Physical, chemical and organoleptic relationships in fresh pork. *Journal of Animal Science*, *19*, 145-149.

Kemp, C. M., Sensky, P. L., Bardsley, R. G., Buttery, P. J., & Parr, T. (2009). Tenderness - An enzymatic view. *Meat Science*, *84*, 248-256.

Koohmaraie, M. (1994). Muscle proteinases and meat aging. *Meat Science*, *36*, 93-104.

Liao, Y.-T., Fan, Y.-X., & Cheng, F. (2010). On-line prediction of fresh pork quality using visible/near-infrared reflectance spectroscopy. *Meat Science*, *86*, 901-907.

Lonergan, S. M., Huff-Lonergan, E., Rowe, L. J., Kuhlers, D. L., & Jungst, S. B. (2001). Selection for lean growth efficiency in Duroc pigs influences pork quality. *Journal of Animal Science*, *79*, 2075-2085.

Lukaski, H. (1996). Biological indexes considered in the derivation of the bioelectrical impedance analysis. *American Journal of Clinical Nutrition*, *64*, 397-404.

Mancini, R. A., & Hunt, M. C. (2005). Current research in meat color. *Meat Science*, *71*, 100-121.

Moeller, S. J., Miller, R. K., Edwards, K. K., Zerby, H. N., Logan, K. E., Aldredge, T. L., Stahl, C. A., Boggess, M., & Box-Steffensmeier, J. M. (2009). Consumer perceptions of pork eating quality as affected by pork quality attributes and end-point cooked temperature. *Meat Science*, *84*, 14-22.

Moeller, S. J., Miller, R. K., Edwards, K. K., Zerby, H. N., Logan, K. E., Aldredge, T. L., Stahl, C. A., Boggess, M., & Box-Steffensmeier, J. M. (2010). Consumer perceptions of pork eating quality as affected by pork quality attributes and end-point cooked temperature. *Meat Science*, *84*, 14-22.

NAMP (2010). *The meat buyers guide* (6th ed.). Reston, VA: North American Meat Processors Association, Thesis.

Nath, T. M. (2008). The use of electrical impedance to rapidly predict beef tenderness. Masters thesis, South Dakota State University.

Norman, J. L., Berg, E. P., Heymann, H., & Lorenzen, C. L. (2003). Pork loin color relative to sensory and instrumental tenderness and consumer acceptance. *Meat Science*, *65*, 927-933.

Price, D. M., Hilton, G. G., VanOverbeke, D. L., & Morgan, J. B. (2008). Using the near-infrared system to sort various beef middle and end muscle cuts into tenderness categories. *Journal of Animal Science*, *86*, 413-418.

Ramsbottom, J. M., & Strandine, E. J. (1948). Comparative tenderness and identification of muscles in wholesale beef cuts. *Journal of Food Science*, *13*, 315-330.

Rust, S. R., Price, D. M., Subbiah, J., Kranzler, G., Hilton, G. G., Vanoverbeke, D. L., & Morgan, J. B. (2008). Predicting beef tenderness using near-infrared spectroscopy. *Journal of Animal Science*, *86*, 211-219.

Shackelford, S. D., Wheeler, T. L., & Koohmaraie, M. (1999a). Evaluation of slice shear force as an objective method of assessing beef longissimus tenderness. *Journal of Animal Science*, *77*, 2693-2699.

Shackelford, S. D., Wheeler, T. L., & Koohmaraie, M. (1999b). Tenderness classification of beef: II. Design and analysis of a system to measure beef longissimus shear force under commercial processing conditions. *Journal of Animal Science*, *77*, 1474-1481.

Shackelford, S. D., Wheeler, T. L., & Koohmaraie, M. (2004). Technical note: Use of belt grill cookery and slice shear force for assessment of pork longissimus tenderness. *Journal of Animal Science*, *82*, 238-241.

Shackelford, S. D., Wheeler, T. L., & Koohmaraie, M. (2005). On-line classification of US select beef carcasses for longissimus tenderness using visible and near-infrared reflectance spectroscopy. *Meat Science*, *69*, 409-415.

Steenkamp, J.-B. E. M., & Van Trijp, H. C. M. (1996). Quality guidance: A consumer-based approach to food quality improvement using partial least squares. *European Review of Agricultural Economics*, *23*, 195-215.

Swantek, P. M., Crenshaw, J. D., Marchello, M. J., & Lukaski, H. C. (1992). Bioelectrical impedance: a nondestructive method to determine fat-free mass of live market swine and pork carcasses. *Journal of Animal Science*, *70*, 169-177.

van Laack, R. L., Stevens, S. G., & Stalder, K. J. (2001). The influence of ultimate pH and intramuscular fat content on pork tenderness and tenderization. *Journal of Animal Science*, *79*, 392-397.

Watanabe, A., Daly, C. C., & Devine, C. E. (1996). The effects of the ultimate pH of meat on tenderness changes during ageing. *Meat Science*, *42*, 67-78.

Wismer-Pedersen, J. (1959). Quality of pork in relation to rate of pH change post mortem. *Journal of Food Science*, *24*, 711-727.

Wright, L. I., Scanga, J. A., Belk, K. E., Engle, T. E., Tatum, J. D., Person, R. C., McKenna, D. R., Griffin, D. B., McKeith, F. K., Savell, J. W., & Smith, G. C. (2005). Benchmarking value in the pork supply chain: Characterization of US pork in the retail marketplace. *Meat Science*, *71*, 451-463.

Wulf, D. M., O'Connor, S. F., Tatum, J. D., & Smith, G. C. (1997). Using objective measures of muscle color to predict beef longissimus tenderness. *Journal of Animal Science*, *75*, 684-692.

Wulf, D. M., & Page, J. K. (2000). Using measurements of muscle color, pH, and electrical impedance to augment the current USDA beef quality grading standards and improve the accuracy and precision of sorting carcasses into palatability groups. *Journal of Animal Science*, *78*, 2595-2607.

Yu, L. P., & Lee, Y. B. (1986). Effects of postmortem pH and temperature muscle structure and meat tenderness. *Journal of Food Science*, *51*, 774-780.

VITA

Kyle Matthew Segner received his Bachelor of Science degree in animal science from Texas A&M University in College Station, Texas in May 2009. He entered the Meat Science program at Texas A&M University in September 2009 and received his Master of Science degree in May 2011. His research interest includes special interest in predicting pork quality with mechanical instruments and teaching in Agrilife Extension programs such as Beef 706 and Beef 101. He plans to publish in the *Journal of Meat Science* with the research that he conducted.

Mr. Segner may be reached at 322 Kleberg Center, 2471 TAMU College Station, TX 77843. His email is k_segner09@hotmail.com or k_segner09@tamu.edu.